



Published in final edited form as:

*Ann Biomed Eng.* 2013 July ; 41(7): 1366–1383. doi:10.1007/s10439-012-0723-0.

## Suggested Connections between Risk Factors of Intracranial Aneurysms: A Review

Juan R. Cebal and Marcelo Raschi

Center for Computational Fluid Dynamics, George Mason University, Fairfax, Virginia

### Abstract

The purpose of this article is to review studies of aneurysm risk factors and the suggested hypotheses that connect the different risk factors and the underlying mechanisms governing the aneurysm natural history. The result of this work suggests that at the center of aneurysm evolution there is a cycle of wall degeneration and weakening in response to changing hemodynamic loading and biomechanic stress. This progressive wall degradation drives the geometrical evolution of the aneurysm until it stabilizes or ruptures. Risk factors such as location, genetics, smoking, co-morbidities, and hypertension seem to affect different components of this cycle. However, details of these interactions or their relative importance are still not clearly understood.

### Introduction

Unruptured intracranial aneurysms occur in 5–8% of the general population<sup>106</sup>. It has been suggested that some aneurysms bleed shortly after formation and thus are rarely detected as unruptured aneurysms, and that most aneurysms without early rupture remain stable through some healing process<sup>112</sup>. Most people with unruptured aneurysms remain asymptomatic and are usually unaware of their presence<sup>143</sup>. Subarachnoid hemorrhage (SAH) from a ruptured cerebral aneurysm is a devastating condition that carries high mortality, long term disability rates and high costs<sup>147</sup>. Increased detection of unruptured intracranial aneurysms, which usually carry low rupture risk, has fueled a decades-long debate of whether aneurysms need immediate treatment or not. Many studies have focused on identifying risk factors for the formation and rupture of intracranial aneurysms as well as on understanding the basic mechanisms responsible for their initiation, progression and rupture.

The underlying mechanisms governing aneurysm evolution from formation to rupture are thought to be multifactorial, involving hemodynamic loads, wall biomechanics, mechanobiology, and contacts with the peri-aneurysmal environment<sup>117</sup>. It is generally accepted that the rupture of saccular aneurysm is the consequence of the inability of the wall to contain the hemodynamic loads and rupture occurs when wall stress exceeds wall strength. However, the detailed mechanisms that weaken the wall and drive the evolution of the aneurysm towards stabilization or rupture are not fully understood.

It has been argued that aneurysms are acquired degenerative lesions originated by the effect of hemodynamic stresses, since aneurysm formation can be produced experimentally by solely augmenting hemodynamic stresses for instance by increasing collateral flow after occlusion of one or more feeding vessels<sup>127</sup>. Presumably, the initial lesion leads to exposure of the collagen and formation of a fibrin matrix that triggers a repair process that remodels the wall of the aneurysm, modifying the geometry and creating aberrant flow conditions in the lumen. The lesion of the endothelium also initiates the development of a thin thrombus lining on the exposed collagen surface, which grows and further changes the geometry and the flow conditions. During the remodeling process, mural cells migrate to the intima and synthesize new collagen matrix while smooth muscle cells infiltrate the luminal thrombus

increasing the strength of the wall and protecting it from rupture. Under these conditions, the unruptured walls present myointimal hyperplasia and thrombus<sup>39</sup>. Luminal thrombosis is known to cause two separate effects leading to lesions on cell walls. First, luminal thrombosis produces high oxidative stress in the wall, accumulating cytotoxic oxidized lipids which trigger cell death. Secondly, these intracellular lipids lead to macrophage infiltration in the aneurysm producing inflammation. Inflammation and matrix degradation processes induce repair mechanisms, such as mural cells migrating to the intima and synthesizing new collagen that counteract the degradative process. In this stage the aneurysm is stable<sup>40</sup>. When there is a loss of mural cells, the repair mechanisms are interrupted and the aneurysm wall matrix degenerates and becomes too fragile to resist hemodynamic pressure and eventually the aneurysm ruptures<sup>65</sup>.

The purpose of this article is to review the current knowledge of aneurysm risk factors and the suggested connections between them and the underlying mechanisms governing the aneurysm natural history. This is not a systematic or a comprehensive review; it highlights some of the effects of different risk factors that have been proposed in the literature. In particular, we will consider the aneurysm location, multiplicity, geometry and hemodynamics, the peri-aneurysmal environment, the vessel wall status, and the patient's genetics and clinical factors.

## Location

### Posterior Circulation

Intracranial aneurysms located in the posterior circulation are less frequent (10–20%)<sup>48, 142</sup> and have been associated with a higher risk of rupture<sup>33, 142</sup> than aneurysms in the anterior circulation. However, the connections between location and differences in risk of rupture remain largely unexplained<sup>142</sup>.

The most common location in the posterior circulation is the tip of the basilar artery (BA), followed by the origin of the posterior inferior cerebellar artery (PICA)<sup>48</sup>. A recent study<sup>125</sup> found that basilar tip aneurysms occur more often with asymmetric artery fusion, which could be related to a more fragile vessel disposition as it is not fully matured or to a possible local increase in the hemodynamic stress in these locations. Aneurysms of the PICA are relatively rare, they account for approximately 2–3% of all intracranial aneurysms and about 18% of all aneurysms in the posterior circulation, but aneurysms in this location have a high rupture rate (approximately 80% are ruptured)<sup>99</sup>.

Aneurysms of the posterior cerebral artery (PCA) are also rare, they account for 1–2% of all cerebral aneurysms and approximately 7% of all posterior circulation aneurysms. Over 30% of them are large or giant, and they often exhibit tumor-like symptoms<sup>41, 144</sup>. They are most commonly located in the P1<sup>114</sup> or P2 segments of the PCA, and have a high degree of coincidence with other vascular lesions such as arterio-venous malformations or multiple aneurysms, suggesting a possible influence of increased hemodynamic stresses on their development.

Aneurysms of the trunk of the basilar artery are rare, they comprise less than 1% of all intracranial aneurysms, however they have high rupture rates (72% ruptured vs. 28% unruptured), high female prevalence (over 80%), and exhibit high degree of multiplicity (approximately 30%)<sup>48</sup>. This could suggest that aneurysm formation at this location is related to vessel wall fragility<sup>48</sup>. Additionally, it has been argued that aneurysms develop at arterial bifurcations due to locally increased hemodynamic stress, so the fact that the basilar trunk does not have any major bifurcation could explain the low incidence of aneurysms in this location<sup>48</sup>.

## Anterior Circulation

Most intracranial aneurysms are located in the anterior circulation. The most common locations for anterior circulation aneurysms are the anterior communicating artery (ACOM) followed by the posterior communicating artery (PCOM), the middle cerebral artery (MCA), and the internal carotid artery (ICA)<sup>33</sup>.

Differences in the size distribution of ruptured aneurysms according to location have been reported<sup>145</sup>. In one study, the rank order of decreasing aneurysm size for ruptured lesion was: ICA-ophthalmic, ICA bifurcation, BA tip, MCA bifurcation, PCOM, ACOM, PICA and distal aneurysms<sup>14</sup>. Another study found the size order of ruptured aneurysms in the Korean population was: BA, MCA, ICA, and anterior cerebral artery (ACA), and observed that many ruptured aneurysms were small (<6mm) suggesting that rupture risk does not depend only on aneurysm size<sup>54</sup>. A study of the Chinese population indicated that most aneurysms occurred in the anterior circulation and that the most common sites for rupture were the ACOM and PCOM, and that a large portion of ruptured aneurysms were small (under 5 mm)<sup>70</sup>. Others showed that aneurysms in the ACA or the ACOM were more often ruptured than unruptured, while aneurysms in the MCA were more often unruptured than ruptured<sup>9</sup>. Another study<sup>95</sup> showed that aneurysms in the ACOM and ACA have an increased tendency to rupture (even small aneurysms under 10 mm), and that ruptured aneurysms were smaller in the ACOM than in the ICA and MCA. Since the diameter of the ACOM and distal ACA are typically smaller than the ICA and MCA, the authors speculated that the size at rupture may be determined by the original wall thickness and diameter of the parent vessel. Similarly, other researchers hypothesize that, according to Laplace's law (which states that the tension required to withstand a given pressure increases with the diameter of a vessel), the critical diameter for rupture is proportional to the average wall thickness. This suggests that aneurysms at smaller arteries may rupture at smaller sizes since they had initially thinner walls<sup>14</sup>. All these observations seem to indicate that rupture risk depends on the location, and that aneurysms at the ACOM and PCOM are more prone to rupture than aneurysms at other locations.

Hypoplasia of the A1 segment of the ACA has been found more frequently in patients with ACOM aneurysms than in those with aneurysms in other locations<sup>67</sup>. Additionally, in patients with ACOM aneurysms larger necks on the dominant side have been observed<sup>68</sup>. These observations led the authors to believe that hemodynamics in the anterior circle of Willis is important for the initiation, growth and rupture of ACOM aneurysms. A study of the flow dynamics in the ACOM complex using in vitro models with idealized geometries showed that geometric changes from a symmetric to an asymmetrical ACOM complex develops cross-flows and high wall shear stress (WSS) at the ACOM artery<sup>136</sup>. This high WSS (about 5 to 10 times larger than the normal range of 10 to 20 dyne/cm<sup>2</sup>) was considered to play an important role for the formation of aneurysms at this location<sup>136</sup>. Another study showed that ACOM aneurysms arise from the dominant side, but are also associated with smaller A1–A2 angle junction of the ACOM complex, where higher hemodynamic stress may occur in patients with normoplastic A1 segments<sup>64</sup>.

Several researchers analyzed the flow dynamics in the ACOM complex. In one study<sup>152</sup>, PIV and LDV techniques were used to analyze the flows in ACOM aneurysms of varying aspect ratios using in vitro models with idealize geometries. In this study, the highest WSS (about 28 dyne/cm<sup>2</sup>) occurred at the aneurysm neck while slow flow and low WSS (below 5 dyne/cm<sup>2</sup>) were observed within the aneurysm sac. The authors suggested that the high WSS at the neck activates platelets and initiates the development of a thrombus that anchors on the dome where very slow flow takes place, inducing inflammation and wall digestion and predisposing the aneurysm for rupture. However, these WSS levels are not higher than those prevailing at branch points in cerebral arteries, where platelet activation does not seem to

normally take place. A computational fluid dynamics (CFD) study<sup>44</sup> with idealized geometries showed that differences in the diameters of the A1 segments of more than 50%, induced high WSS in the ACOM artery (25–70 dyne/cm<sup>2</sup>), suggesting a possible explanation to why ACOM aneurysms are more frequent and more prone to rupture than aneurysms in other locations. An image-based CFD study indicated that asymmetric geometries of the ACOM complex or asymmetric ICA flow waveforms can significantly affect the complexity and stability of flow patterns within ACOM aneurysms<sup>17</sup>. This study also highlighted the importance of considering the patient-specific geometry of the ACOM complex including both avenues of flows when analyzing the flow dynamics of ACOM aneurysms<sup>16</sup>. A subsequent study based on 26 patient-specific CFD models found that ruptured ACOM aneurysms had on average about 2.3 times higher maximum WSS than unruptured aneurysms at this location, and that asymmetric flow division at the aneurysm neck was more common in ruptured aneurysms<sup>18</sup>. In another CFD study<sup>57</sup>, cross flows (flows with opposite directions) were observed in bilateral ACOM arteries, depending on the symmetry of the ICA flow waveforms. These cross flows induced high WSS (65–185 dyne/cm<sup>2</sup>) in the ACOM artery, which could play a role in aneurysm development. All these studies and observations seem to suggest that abnormal flow conditions and high WSS in particular, play an important role in the development and rupture of ACOM aneurysms.

Studies of ACA aneurysms showed that aneurysms in the A1, A2 or distal ACA (A3 or beyond) are rare, comprising less than 1% of all aneurysms<sup>35, 76, 78</sup>. These studies also showed that these aneurysms often occur at the origin of perforators, have thin walls, have high multiplicity (although mirror aneurysms are rare), are frequently associated with vascular anomalies of the circle of Willis, and rupture at smaller sizes than aneurysms at other locations. These observations led the authors to suggest that fragile thin walls and abnormal hemodynamics play an important role in the development and rupture of aneurysms at these locations.

The ICA is the most common site for unruptured intracranial aneurysms, about 38% of all unruptured aneurysms are found in this artery<sup>32</sup>. PCOM aneurysms have high prevalence; they comprise approximately 25% of all intracranial aneurysms and about 50% of all aneurysms of the ICA<sup>47</sup>. True PCOM aneurysms (those arising purely from the PCOM artery, not its junction to the ICA) constitute about 10% of all PCOM aneurysms. They tend to be smaller than junctional PCOM aneurysms, but have similar prevalence of rupture, which may indicate a higher rupture risk. Additionally, larger ipsilateral P1 and P2 segments of the PCA have been observed in association with true PCOM aneurysms, consistent with larger flows and higher WSS through the PCOM artery<sup>47</sup>. A CFD study<sup>7</sup> using four patient-specific geometries of aneurysms and infundibulae at the PCOM artery origin in the ICA observed flow impingement at the distal wall and creation of a region of elevated pressure (4–5 mmHg) surrounded by a band of high WSS (200–300 dyne/cm<sup>2</sup>). The authors suggest these regions coincide with sites of rupture of the infundibulae or progression to aneurysms, and that once the aneurysms form at this location flow impinges at the dome of the aneurysm and near the location of secondary blebs.

A study<sup>79</sup> of aneurysms located at the origin of the anterior choroidal in the ICA showed that they are rare, comprising 2–5% of all intracranial aneurysms. Surgical observations made in this work indicated that they are small, with thin walls, and usually one or more arteries originate at their base. They have high multiplicity; about 60% have multiple aneurysms, usually in the ipsilateral PCOM or MCA. In about 14% of the cases the PCOM is absent. They have relatively low rupture rates (about 60% are unruptured while 40% ruptured), and many of the ruptured aneurysms are small (less than 7 mm). The authors argue that high multiplicity and thin walls suggests fragile walls, while missing PCOM or

coincidence with other ipsilateral aneurysms suggests higher flows and increased hemodynamic stress.

A recent study compared aneurysms at the internal carotid artery bifurcation with aneurysms at the tip of the basilar artery<sup>142</sup>. The results showed that aneurysms are less frequent at the ICA bifurcation than at the BA tip, and the proportion of ruptured to unruptured aneurysms is smaller in the ICA bifurcation than in the BA bifurcation. Since there are two ICA bifurcations for every BA bifurcation, the authors argued for a lower risk of rupture at the ICA bifurcation, and speculated that hemodynamics is not a likely explanation for the higher risk of posterior circulation aneurysms. Another study compared the flow dynamics in ICA and MCA bifurcations using experimental in vitro models with patient-specific geometries<sup>133</sup>. The velocity profile approaching the ICA bifurcation was found to be flattened due to the bends of the carotid siphon making the hemodynamic stress (pressure, tension, shear stress) lower than at the MCA bifurcation where the profile was sharpened. The authors suggested that this effect could explain the lower incidence of aneurysms at the ICA bifurcation than at the MCA bifurcation. Another study<sup>109</sup> found that aneurysms of the ICA bifurcation were deviated to the side of the A1 segment of the ACA, and speculated that this could be explained by the fact that on this side the artery might suffer higher hemodynamic stress.

Two studies of aneurysms at the peri-ophthalmic internal carotid artery used CFD modeling to compare the hemodynamics of ruptured and unruptured aneurysms at this location. They concluded that hemodynamics and WSS can be different between ruptured and unruptured aneurysms despite similar size and anatomical location<sup>29</sup>. Furthermore, relative WSS was about 1.75 times higher in ruptured than in unruptured aneurysms, while WSS in the parent arteries was similar<sup>28</sup>. In contrast, a study of 26 aneurysms in the paraclinoid and supraclinoid ICA found that ruptured and unruptured aneurysms had similar maximal WSS, but ruptured aneurysms had a larger area under low WSS (27% vs. 11%, defined as 10% below the average WSS in the parent artery)<sup>58</sup>.

Aneurysms of the middle cerebral artery are common; about 20% of all intracranial aneurysms are found at this location. Most MCA aneurysms are located at the MCA bifurcation. Main trunk involvement is rare and aneurysms arise at early branches with a superior orientation consistent with the origin of perforators<sup>97</sup>. Distal MCA aneurysms are uncommon (less than 2–5% of all aneurysms), they tend to rupture at smaller sizes, and they are mostly fusiform with etiologies of infection or trauma<sup>55</sup>. A CFD study using 20 patient-specific models revealed that compared to the average WSS in the parent vessel (36 dyne/cm<sup>2</sup>), the WSS was high at the neck of MCA bifurcation aneurysms (143 dyne/cm<sup>2</sup>) and low at the tip of ruptured aneurysms (16 dyne/cm<sup>2</sup>), inducing the authors to think that low WSS may facilitate growth and trigger aneurysm rupture<sup>123</sup>. Another CFD study of 24 aneurysms at different locations showed that WSS and aneurysmal inflow rate changed with location, being higher in the MCA and lower in the BA and ACOM arteries<sup>26</sup>.

### Circle of Willis

It has been shown that ACOM, PCOM and BA tip aneurysms tend to occur more often in anatomically variant circle of Willis<sup>125</sup>. ACOM aneurysms are found more frequently together with unilateral aplasia of A1 segments of the ACA, followed with hypoplasia and least commonly in a fully developed ACOM complex. PCOM aneurysms tend to occur more frequently with large sized PCOM arteries, and BA tip aneurysms are usually found in asymmetric BA bifurcations. All this evidence may relate to more fragile wall disposition as it is not fully matured, or to altered hemodynamics secondary to the anatomical variation. A cadaveric study of the mestizo population in Colombia showed that aneurysm prevalence was associated to asymmetric configuration of the circle of Willis<sup>104</sup>. The most common

variation was hypoplasia of the PCOM, which highlights the importance of the effects of hemodynamic dominance. A later paper argued that the architecture of the circle of Willis seems to influence the distribution of hemodynamic forces, but that aneurysm pathogenesis is still not well understood<sup>92</sup>.

Saccular aneurysms usually arise at the distal carina of arterial bifurcations, where the vessels are exposed to maximum impact of WSS<sup>126</sup>. The magnitude of the WSS depends on the geometry of the bifurcation, and is minimum when the relation between radii and angles follows the principle of minimum work given by Murray's law<sup>89, 90</sup>. However, it has been argued that although the distal arterial branches follow the principle of minimum work, the circle of Willis does not, which could explain the higher prevalence of aneurysms in bifurcations with larger angles<sup>2</sup>. A CFD model of the circle of Willis constructed from population averaged characteristics showed that high WSS (>300 dyne/cm<sup>2</sup>) occurred at locations where aneurysms are frequently seen and in anatomic variations known to have increased risk of aneurysm development. Another paper argued that the circle of Willis influences the development of intracranial aneurysms, and studied whether it also affects the risk of rupture<sup>36</sup>. The authors concluded that the configuration of the circle of Willis was not strongly correlated to rupture, but that moderate risk could not be excluded. A more recent study showed that anomalies of the circle of Willis were more frequently found in ruptured than in unruptured aneurysms of the ACOM or PCOM arteries<sup>75</sup>. Thus, the authors speculate that increased flow in combination with vascular configurations that do not minimize the energy expenditure at bifurcations may, via turbulent flows and increased WSS, contribute to intracranial aneurysm formation and progression.

## Peri-Aneurysmal Environment

Contacts between the aneurysm and extra-vascular anatomical structures of the peri-aneurysmal environment (PAE) have been suggested as potential factors affecting the rupture risk of intracranial aneurysms. Computer models with idealized geometries have been used to propose that smooth contact constraints provide protective support to the aneurysm dome by decreasing the wall stresses near the fundus, while increased wall stresses can be created by sharp contacts or near the borders of contact regions where the wall can undergo sharp bends or deformations<sup>115</sup>.

Imaging studies have focused on the topographic relationship between the aneurysm and the cisternal compartment of the peri-aneurysmal environment. In one study<sup>129</sup>, the presence of contacts between the aneurysm and surrounding structures such as bone, dura, brain cranial nerves, arteries and veins were identified in MR, CT and DSA images. It was found that the perianeurysmal environment had a significant influence on aneurysmal rupture pattern, whenever the aneurysm was in direct contact with extravascular structures. The aneurysm shape and likely rupture point (blebs in particular) were influenced by the PAE. This was confirmed in another study that found marked and minor deformations and blebs in regions confronted or adjacent to contacts with PAE structures<sup>113</sup>. Another study suggested that contact with the environment is an additional determinant of the aneurysm evolution and its risk of rupture<sup>110</sup>. A similar study<sup>111</sup> found that, compared to unruptured aneurysms, ruptured aneurysms were larger and more irregular, were more likely to develop contact constraints with the PAE, and showed higher rates of unbalanced constraints. Ruptured aneurysms tended to be located in regions with more constraining PAE's, and irregular shapes were correlated with unbalanced contact constraints.

Interestingly, a study of ruptured distal ACA aneurysms based on surgical observations<sup>77</sup> showed that most of these aneurysms are located at the pericallose artery (A3 segment) and embedded between the two cerebral hemispheres. The authors suggested that these

aneurysms tend to rupture at smaller sizes and are associated with higher rates of intra-cerebral hemorrhage than aneurysms in other locations, possibly due to the narrow space provided by the pericallose cistern, i.e. a more constraining PAE than other locations. In contrast, a study of aneurysms in the cavernous internal carotid artery<sup>66</sup> found that aneurysms at this location are typically large, have a low rupture rate, and rupture at larger sizes than aneurysms in other locations. The authors suggested that these observations could be explained by a protective PAE at this location.

Finally, a recent case study of a growing aneurysm analyzed with image-based CFD modeling showed that in some cases contacts with structures of the PAE such as bone can significantly affect the shape and geometrical evolution of the aneurysm and can alter the hemodynamic loads as the aneurysm grows<sup>119</sup>.

## Multiplicity

Multiple aneurysms occur in approximately 20–30% of patients with intracranial aneurysms<sup>6, 81</sup>. Mirror aneurysms (occurring at the same locations bilaterally) are found in about 9% of the population, but multiple mirror aneurysms are very rare<sup>6</sup>. In general, researchers seem to believe that multiplicity of cerebral aneurysms is indicative of weaker or more fragile walls throughout the vascular trees. However, as discussed before some locations have higher rates of incidence of multiple aneurysms. Perhaps this could indicate that a combination of fragile walls and increased hemodynamic stress secondary to increased flow in certain vessels around the circle of Willis would give rise to multiple lesions along the affected vascular tree.

A case study of multiple aneurysms in the internal carotid artery seems to give support to this idea<sup>42</sup>. This report describes the treatment of a giant ICA cavernous aneurysm and two supraophthalmic ICA aneurysms via parent artery occlusion. After balloon occlusion of the ICA proximal to the giant cavernous ICA aneurysm, flow reversal in the ICA and flow to the ophthalmic artery and the supra-ophthalmic aneurysms via collateralization through the PCOM and the ACOM were observed. Subsequently, thrombosis and regression of the two supraophthalmic aneurysms sizes were observed. The authors then suggested that changes in the cerebral hemodynamics can lead to plastic changes in the vessel architecture.

In contrast, a case study of a patient with mirror aneurysms in which a de novo aneurysm developed and ruptured<sup>53</sup> argued that the mechanism of development of multiple aneurysms, especially mirrors, cannot be explained based only on hemodynamic factors and congenital segmental arterial vulnerability which is generalized rather than focal is highly likely.

Additionally, another study suggested that multiple aneurysms could arise as consequence of developmental defects in embryological territories that affect vascular segments<sup>13</sup>. A different study<sup>15</sup> argued that multiple vascular lesions raise the hypothesis that these patients have a strong congenital predisposition for intracranial aneurysms or a significantly higher exposure to acquired risk factors. In their study the authors found differences in the relative prevalence of risk factors between multiple and pure mirror aneurysms, and suggested that this observation provides support to the hypothesis of a different etiologic process occurring in mirror aneurysms.

A study based on image-based CFD compared the hemodynamics between the ruptured and the unruptured aneurysm in 9 pairs of mirror aneurysms<sup>81</sup>. It was found that the ruptured aneurysms had more irregular WSS distributions, a larger portion of the aneurysm sac under low WSS (12.2 % vs 3.96%, defined as  $WSS < 15 \text{ dyne/cm}^2$ ) and higher oscillatory shear index (OSI). This suggests that controlling for genetics, location and other patient-specific

risk factors, the hemodynamic loading of the aneurysm can have a significant influence on its rupture potential.

## Geometry

### Size

The data of the International Study of Unruptured Intracranial Aneurysms (ISUIA), one of the largest studies of aneurysm risk, indicated that aneurysm size and location have a significant role in determining the risk of future rupture of intracranial aneurysms<sup>148</sup>. This study identified asymptomatic small aneurysms (< 7 mm) located in the anterior circulation as the lowest-risk natural history group. Similarly, a meta-analysis of data from unruptured aneurysms longitudinally suggested that the relative rupture risk of aneurysms larger than 10 mm compared to aneurysms smaller than 10 mm were over 5 times higher<sup>33</sup>. In contrast, other studies found no significant differences in the size of ruptured and unruptured aneurysms, i.e. no size threshold at which the frequency of ruptured aneurysms increased abruptly, and also no difference in the proportion of ruptured to unruptured aneurysms for sizes below 7 mm or below 10 mm<sup>9</sup>. In contrast to the ISUIA, this study also observed that most small aneurysms, both ruptured and unruptured aneurysms smaller than 7 mm, are located in the anterior circulation. This led the authors to conclude that size is not the most important determinant of aneurysm rupture risk, as many anterior circulation aneurysms do rupture. Similarly, another study of ruptured aneurysms concluded that many small aneurysms (<5 mm) do rupture, and that many small aneurysms are associated with large SAH volumes<sup>97</sup>. In a subsequent study most ruptured aneurysms were less than 7 mm in size (mean diameter was 6.28 mm), and about 72% of ruptured aneurysms were smaller than 7 mm in diameter and 88% smaller than 10 mm<sup>56</sup>. Based on location the data also showed that ACOM aneurysms most often presented with rupture sizes less than 7 mm (77%) and 10 mm (92%) in diameter. Additionally, symptomatic aneurysms are often large and produce a mass effect, and it is difficult to separate size from being symptomatic as independent factors<sup>5</sup>.

On the other hand, studies of giant intracranial aneurysms showed that although they have a relatively low incidence (about 5% of all aneurysms) they have a high rupture risk; rupture rate is over 50% and mortality is over 60% in two years<sup>31, 102</sup>. Most giant aneurysms present with symptoms in the form of SAH, mass effect (the most common symptom), cerebral ischemia, and embolic events<sup>102</sup>. Giant aneurysms have a predilection for cavernous and proximal ICA, followed by the ophthalmic artery, and the MCA. Two thirds occur in the anterior circulation and one third in the posterior circulation. In the posterior circulation, most giant aneurysms are located at the tip of the BA and the P1 segment of the PCA, mid basilar and vertebra-basilar junction are less frequent, and most aneurysms at these latter locations are fusiform. This is a heterogeneous group that includes saccular as well as fusiform aneurysms from atherosclerotic origin. Giant saccular aneurysms are thought to develop by gradual enlargement of small saccular aneurysms by repeated endothelial damage from turbulent flow and subsequent healing of the wall, while giant fusiform aneurysms are thought to develop from atherosclerotic degeneration of the wall<sup>31</sup>.

### Shape

Aneurysm shape has been proposed as an important factor for the assessment of aneurysm rupture risk in several studies. For instance, the aspect ratio (AR) between ruptured and unruptured aneurysms was found to be significantly different, with almost 80% of ruptured aneurysms having AR>1.6 while almost 90% of unruptured aneurysm having AR<1.6<sup>137</sup>. This study proposed that the aspect ratio may be useful in predicting imminent aneurysmal



ruptures, and suggests that larger aspect ratios are associated with slower flows that induce thrombosis and wall degeneration.

Subsequently, irregular multilobular appearances were found to be significantly more common in ruptured aneurysms with sizes between 5 and 9 mm<sup>10</sup>. Similarly, non-spherical shapes (oval, oblong and multilobulated) were found to be associated with rupture<sup>36</sup>. Additionally, aneurysms where the flow from the parent artery enters straight into the aneurysm (determined by looking at the angle between the aneurysm and the parent artery axis) were also associated with rupture<sup>36</sup>. In another study, shape descriptors or indices based on geometric moment invariants were shown to be better predictors of aneurysm rupture state than AR or size<sup>88</sup>. Later, univariate and multivariate statistical analyses showed that Zernike moment invariants computed on the aneurysm sac and a small portion of the parent artery were better predictors of rupture of MCA aneurysms than other geometric descriptors such as size, neck, depth, surface area, volume, and aspect ratio<sup>141</sup>. Other researchers proposed the entropy of the centroid radii model as a descriptor of the aneurysm shape and a discriminator of aneurysm rupture status. They analyzed sidewall and bifurcation aneurysms separately and found a classification accuracy of 80% and 70%, respectively<sup>71</sup>. Similarly, the use of the writhe number, which measures the extent to which a curve twists and coils around itself, to characterize aneurysm shapes and predict aneurysm rupture status resulted in approximately 86% accuracy for sidewall aneurysms and 71% accuracy for bifurcation aneurysms<sup>74</sup>.

### Geometric Indices

Many studies have focused on identifying sets of geometric indices to discriminate between ruptured and unruptured aneurysms. Various indices, their physical interpretations, and possible role as prognosticators for rupture risk are discussed in<sup>82</sup>.

A comparison of ruptured and unruptured aneurysms in the same patients found that size and AR were significantly different between these two groups<sup>91</sup>. The authors argued that the larger the AR, the slower the intra-aneurysmal flow, and that the higher risk for larger AR could be explained because slow flows were thought to be associated with higher risk due to a higher propensity for degenerative processes at the wall. Another study found that maximum diameter, height, maximum width, bulge height, parent artery diameter, aspect ratio, bottleneck factor and aneurysm/parent artery ratio were significantly associated to rupture<sup>49</sup>. Multivariate statistics showed that bottleneck factor and high-width ratios were consistently associated with rupture<sup>49</sup>. Similarly, statistical differences were found between mean values in ruptured and unruptured aneurysm groups for size ratio, undulation index, non-sphericity index, ellipticity index, aneurysms angle, and aspect ratio. Size ratio and aneurysm angle were highlighted as parameters that take into account the vessel geometry and thus could bridge the gap between morphological studies and qualitative location based studies<sup>37</sup>.

In order to understand the effects of size ratio on aneurysmal flow, a sidewall and a terminal aneurysm were analyzed with CFD<sup>135</sup>. It was observed that higher size ratio, irrespective of aneurysm type and absolute aneurysm or vessel size, gives rise to flow patterns typically observed in ruptured aneurysms. The authors concluded that these results provide hemodynamic support for the existing correlation between size ratio and aneurysm rupture. Similarly, CFD studies of 34 saccular aneurysms suggested a linear correlation between the spatial average of WSS and an area index computed as the ratio of the aneurysm area and the artery area at the model inlet<sup>139, 140</sup>.

Other studies analyzed the ability of geometric indices and their combinations to discriminate ruptured from unruptured aneurysms. A logistic regression model using

aneurysm height, width and neck size identified aneurysm rupture status with good accuracy (83% sensitivity and 80% accuracy)<sup>101</sup>. A binary logistic regression model using aspect ratio and size ratio showed good sensitivity (approximately 84%) and specificity (about 66%)<sup>154</sup>. Logistic regression was used to evaluate the independent predictive value of maximum size and size ratio, only size ratio remained in the final predictive model<sup>105</sup>. Aspect ratio, bottleneck ratio, height-width ratio, and volume-to-neck area ratio were found to be correlated to rupture status<sup>108</sup>. Volume-to-ostium ratio showed better discrimination for aneurysm rupture status than size and AR<sup>153</sup>. More recently, it has been reported that size ratio is not useful for bifurcation aneurysms and that the incremental contribution of the size ratio over height or maximum diameter could not be validated for sidewall aneurysms<sup>72</sup>. Similarly, AR, height-width and bottleneck factor were shown to depend on parameter definition, thus it was concluded that adoption of a standard methodology and sizing nomenclature seems critical to ensure a reproducible rupture prediction<sup>73</sup>. A comparison of aneurysm geometry with a bounding sphere revealed a trend associating the ratios of aneurysm volume and surface area with rupture<sup>27</sup>. In another study, AR over 1.6, dome diameter over 10 mm, a deviated neck, and right-sidedness were independently associated with aneurysm rupture in a large retrospective cohort<sup>3</sup>.

Deviation of the aneurysm neck was most commonly observed in ruptured than unruptured terminal aneurysm, and CFD analyses showed that this neck deviation caused flow separation and stagnation within the aneurysm<sup>96</sup>. Additionally, a CFD study of 42 terminal aneurysms showed that asymmetric flow patterns splitting from the parent artery and sliding along the side wall of the aneurysms and producing regions of elevated WSS were more common in ruptured than unruptured aneurysms<sup>19</sup>. Finally, ruptured aneurysms were found to have more obtuse angles (more aligned with the parent artery axis, i.e. aligned with the flow) than unruptured aneurysms and a CFD analysis with idealized geometrical models showed that increasing angle, the flow exhibits higher jet velocity and kinetic energy as well as higher WSS and WSS gradients<sup>8</sup>. Another CFD analysis of 21 patient-specific models showed that aneurysms with an axis parallel to the parent artery have a tendency to have a jet flow pattern and uneven distribution of unsteady pressure. The authors pointed out that these aneurysms may have a higher rate of rupture as than those with a main axis perpendicular to the parent artery<sup>131</sup>.

## Hemodynamics

Hemodynamics has been proposed for many years as a fundamental player in the process of aneurysm formation and progression. An early review of the supporting evidence of the theory of congenital etiology of saccular aneurysms concluded that there is no evidence of a congenital, developmental, or inherited weakness of the wall; and that the most plausible explanation is that aneurysms are acquired degenerative lesions caused by hemodynamic stress<sup>127</sup>. The authors explained that the mural atrophy leading to aneurysm development can be produced experimentally by hemodynamics alone. Occlusion of one or more feeding vessels may enhance the possibility of aneurysm formation at arterial bifurcations subjected to augmented hemodynamic stress associated to collateral flow. Hypertension and connective tissue disorders associated with acquired loss of tensile strength of the connective tissues are not essential; they seem to be aggravating rather than causal factors. Another study explains that saccular cerebral aneurysms are induced in rats by ligation of one or both of the common carotid arteries, experimental hypertension, and beta-aminopropionitrile feeding<sup>43</sup>. Combination of ligation of the carotid artery and experimental hypertension induce aneurysms within a few months by increasing hemodynamic stress. Beta-aminopropionitrile makes the arterial wall fragile, increasing the incidence of aneurysmal development. They observed that aneurysms are strongly related to increased

hemodynamic stress, are located on the large arteries at the base of the brain, and some originate from the apex of bifurcations.

Later, a study using 2D CFD simulations of idealized aneurysm models in curved and bifurcating arteries showed increased WSS, pressure and impulse at the apex of bifurcations and outer wall of curved vessels<sup>38</sup>. The authors concluded that in the absence of any underlying disease process aneurysm development is a mechanically mediated event. Another study explains that congenital aneurysms, which are mainly observed at branching sites in the circle of Willis, are developed as a consequence of mechanically-induced degeneration of the wall internal elastic lamina with a genetic predisposition in the form of a wall structure deficiency in frequent familial context<sup>11</sup>. In this same study, high pressure zones were observed in CFD models, especially of terminal aneurysms; and the authors suggest that the greater the pressure, the greater the risk of aneurysm rupture. But, they also raise the question of whether the sites of high wall tension susceptible to rupture coincide with regions of high pressure.

More recently, it has been shown that a combination of high WSS ( $>1220$  dyne/cm<sup>2</sup>) and positive wall shear stress gradient (WSSG) ( $>5300$  dyne/cm<sup>2</sup>/mm) produced by bilateral common carotid artery ligation induce aneurysm formation at the terminus of the basilar artery in rabbit models<sup>87</sup>. Subsequently, it has been suggested that some risk factors such as smoking, alcohol and cocaine consumption, are thought to induce aneurysm formation via mechanisms that increase blood pressure and hemodynamic stresses<sup>100</sup>. After the aneurysm has formed, complex hemodynamic flow patterns are thought to play a role in its continued growth and eventual rupture. Local pathological alterations of hemodynamic forces can injure the vascular lining inducing inflammatory responses that result in vascular smooth muscle cell apoptosis and migration and endothelial cell remodeling.

Several CFD based studies have proposed different indices as markers of regions prone to aneurysm formation such as the aneurysm formation indicator (AIF)<sup>84</sup> or the gradient oscillatory number (GON)<sup>121</sup>. However, it is still not clear if these variables can reliably identify local hemodynamic conditions that lead to aneurysm initiation<sup>116</sup>.

Since associations between aneurysm rupture and irregular shapes and in particular the presence of blebs or secondary lobulations have been reported, several studies have investigated possible relationships between local hemodynamics and the formation of blebs in intracranial aneurysms. An in vitro LDV study in two realistic models of an MCA and a BA tip aneurysm showed nonuniform WSS distribution in the aneurysm walls and regions exposed to relatively high WSS. Blebs of both aneurysms were exposed to high WSS, and unlike previous idealized studies, the inflow zone was not exposed to high WSS<sup>134</sup>. Similarly, high resolution PC-MR in 2 realistic in vitro models of BA and MCA bifurcation aneurysms revealed that a bleb region in the BA tip and a dome region in the MCA aneurysm were consistently exposed to higher WSS within a small local area with high spatial variation and little temporal change in comparison to other aneurysmal regions<sup>1</sup>. Another study, using mathematical models of the wall mechanics, proposed the formation of blebs as a likely path to aneurysm rupture<sup>86</sup>. The authors suggested that the formation of daughter aneurysms temporarily decreases the wall tension protecting the aneurysm from imminent rupture, until further growth elevates the tension leading to rupture. Later, a patient-specific CFD study of the development of small blisters in three aneurysms longitudinally followed suggested that low WSS magnitude ( $<10$  dyne/cm<sup>2</sup>) may trigger aneurysm progression and that blister formation is associated with high WSS gradient in the large region of low WSS<sup>122</sup>. In contrast, a CFD study of 30 blebs in 20 aneurysms showed that most blebs occurred at or adjacent to regions previously exposed to the highest WSS

and were aligned with the inflow stream<sup>25</sup>. This study also suggested that once blebs form they develop counter circulation vortices and progress to a state of lower WSS.

Numerous studies have compared the hemodynamics of ruptured and unruptured aneurysms. A study of 53 patient-specific geometries argued that wide-necked aneurysms or those with wide-caliber draining vessels are high flow lesions that tend to rupture at larger sizes, and that small-necked aneurysms or those with small-caliber draining vessels are low flow lesions that tend to rupture at smaller sizes<sup>45</sup>. Another study based on 62 patient-specific CFD models observed that concentrated inflow jets, small regions of flow impingement, complex and unstable flow patterns were more frequent in ruptured than unruptured aneurysms<sup>20</sup>. Subsequently, two case studies of aneurysms imaged immediately before they ruptured confirmed that these qualitative characteristics were present in these two aneurysms which were obviously at high risk of rupture<sup>21, 118</sup>. Later studies based on 210 CFD models confirmed these trends<sup>24</sup>, and defined quantitative indices such as maximal WSS, the inflow concentration index (ICI), shear concentration index (SCI), and viscous dissipation ratio (VDR) that were found to be higher (except for VDR which was lower) in ruptured than in unruptured aneurysms<sup>23</sup>.

Another study<sup>59</sup> defined a flow impingement index (IMI) and showed that the maximum WSS increased with the IMI but the area of high WSS (defined as the region where  $WSS > 0.5 * \max WSS$ ) is not proportional to the size of impingement. Additionally, this study showed that there is a time delay between the flow impingement and the peak flow in the parent artery, which depends on the aneurysm size and heart rate<sup>59</sup>.

In a recent study of one MCA aneurysm, non-laminar flow behavior was observed, and it was concluded that turbulence can be present in intracranial aneurysms, causing increased WSS magnitude, increased frequency at which the WSS vector changes direction, and local pressure fluctuations; however it is unknown how these effects would alter cell remodeling and affect the wall<sup>138</sup>.

As mentioned before, CFD studies of ACOM aneurysms<sup>18</sup>, ophthalmic artery aneurysms<sup>29</sup>, and terminal aneurysms<sup>19</sup> showed that ruptured aneurysms had on average higher WSS than unruptured aneurysms. In contrast, other studies found that ruptured aneurysms were under lower WSS<sup>123</sup> and had larger areas under low WSS than unruptured aneurysms<sup>58, 139</sup>. In another study, multivariate logistic regression analysis of morphological (size ratio, undulation index, ellipticity index, non-sphericity index) and hemodynamic parameters (average WSS, maximal WSS, low WSS area, average OSI, number of vortices, relative residence time) in 119 patient-specific CFD models identified WSS, size ratio and OSI as independent discriminants of aneurysm rupture status<sup>150</sup>. It has recently been argued that apparent discrepancies in CFD findings<sup>63</sup> arise from simplistic univariate analysis that can be resolved with multivariate analysis<sup>149</sup> and multi-population multi-center data<sup>22, 107</sup>.

Finally, studying aneurysm growth is important because aneurysm rupture has been significantly associated with aneurysm growth during follow up<sup>30, 61</sup>. A few studies have compared the hemodynamics of growing and stable aneurysms longitudinally followed. One study compared a growing aneurysm to a stable aneurysm and observed abnormally low WSS ( $< 10 \text{ dyne/cm}^2$ ) in the region where the aneurysm grew<sup>60</sup>. Similarly, another study analyzed seven growing aneurysms and concluded that aneurysmal growth occurs at regions of abnormally low WSS<sup>12</sup> ( $< 7 \text{ dyne/cm}^2$ ). Another study considered 9 growing aneurysms and 16 stable ones and observed that complex, unstable flow patterns and concentrated inflows were more common in growing aneurysms, and that growing aneurysms had lower viscous dissipation ratios, higher maximum WSS, lower minimum WSS, larger areas under low WSS, and larger OSI<sup>120</sup>. Another CFD study of two growing tandem aneurysms of the

PICA showed that the proximal multilobular aneurysm had high flow and physiological levels of WSS (4.5–12 dyne/cm<sup>2</sup>) in the region of growth, whereas the distal rounded aneurysm had low flow and low WSS (0.2–4.5 dyne/cm<sup>2</sup>) in the growing sac<sup>130</sup>. This study suggested that the growing region of an aneurysm could be exposed to either high WSS at the inflow zone or to low WSS and high OSI in the aneurysm sac.

Other studies compared the hemodynamics in stable aneurysms and in aneurysm that ruptured during the observation period. One such study compared 6 ruptured aneurysm to 26 stable aneurysms and found that the so called energy loss coefficient (EL) was higher in the ruptured group, but WSS was similar between the two groups<sup>103</sup>. Additionally, flow visualizations suggested that although the mean average inflow speed of ruptured aneurysms was 2 times higher than that of the stable aneurysms, the flow inside ruptured aneurysms appeared to undergo longer resident tracks, with stronger impact on the aneurysm wall. On the contrary, the flow inside stable aneurysms passed smoothly through the aneurysms. A second study analyzed 50 ICA aneurysms (6 ruptured during observation) and 50 MCA aneurysms (7 ruptured during observation) and concluded that a pressure loss coefficient (PL) was smaller in the aneurysms that ruptured for both locations, minimum WSS was lower for ruptured aneurysms in the ICA but not in the MCA, and average WSS, maximum WSS, OSI and EL were not significantly different between the two groups<sup>132</sup>.

## Vascular Wall

Hemodynamic studies provide information and describe the blood flow environment within the aneurysms and the loads on the aneurysm walls. This is important because it is thought that these loads and hemodynamic conditions induce mechano-biological changes in the wall structure that tend to weaken and degenerate the wall thus provoking aneurysmal progression towards rupture. However, as shown by a study based on idealized structural models of aneurysms, the shape of the aneurysm, its material properties as well as the loading, not just its size, are important factors that affect the distribution of stresses and strains within the wall<sup>69</sup>.

Previous studies based on anatomical and histological observations reported on the site of aneurysm rupture. One such study reported that 57% of ruptures involve the dome, 33% involve the middle part of the aneurysm, and 10% the neck<sup>93</sup>. Others have reported that 84% of ruptures involve the dome, 14% involve the wall, and 2% involve the neck<sup>146</sup>. An in vitro study of two ruptured aneurysms using patient-specific geometries from cadaveric data showed that in these aneurysms the flow entered through the distal neck and impacted on the distal side wall, where the aneurysms had ruptured<sup>50</sup>.

Subsequently, fluid-structure interaction models using patient-specific geometries were used to estimate the distribution of wall stresses. One such study analyzed the wall stress in an aneurysm located in the MCA bifurcation assuming uniform distributions of wall thickness and material properties<sup>51</sup>. A region of high wall tension ( $5 \times 10^6$  dyne/cm<sup>2</sup>) was observed at the fundus of the aneurysm; where it is believed that aneurysms usually rupture.

Determining unambiguously the site of rupture of cerebral aneurysms is challenging. One study used cardiac-gated dynamic CTA to image aneurysm wall pulsation in vivo<sup>46</sup>. In ruptured aneurysms, the bleeding site was considered to correspond to the area of observed pulsation, and in unruptured aneurysms, the detection of pulsation was associated with subsequent change in shape in follow up exams. Although previous studies have reported that it is very likely for a bleb to be the bleeding site<sup>83</sup>, determination of the rupture site through dynamic imaging of wall pulsation in clinical cases indicate that this is not always true.

It has been suggested that the point of aneurysmal rupture is the thinnest part of the aneurysm wall<sup>52</sup>. A recent study based on mechanical testing of aneurysm tissue harvested during surgical clipping demonstrated three main tissue classes: soft, rigid and intermediate<sup>34</sup>. The analysis had to be performed for each gender separately, and tissue was found to be on average more rigid in unruptured aneurysms than in ruptured aneurysms within each gender subgroup. Additionally, it was reported that wall thickness was not correlated to the rupture status. On the other hand, other studies have tried to image the wall thickness in vivo. One study used black blood MRI techniques and reported that the neck region is thicker than the dome region, and had similar (or even higher) thickness to the adjacent parent artery<sup>98</sup>. Another study described intra-operative estimations of the wall thickness, and indicated that the dome of unruptured aneurysms is highly heterogeneous with areas of variable thickness that appear to be related to the process of aneurysm development<sup>62</sup>. It was argued that these inconstant properties affect wall tensile stress and may play a role in aneurysm pathogenesis and focal rupture. Interestingly, it was also observed that small aneurysms have a larger portion of thin wall than larger aneurysms.

## Genetics

Some hereditary disorders that cause vascular abnormalities, such as Autosomal Dominant Polycystic Kidney Disease (ADPKD) or Ehlers-Danlos Syndrome (EDS) Type IV, have been associated with intracranial aneurysms or aneurysmal SAH. Aneurysm prevalence in ADPKD has been estimated at approximately 5 times that in the general population<sup>94</sup>. Growth and rupture risks have not been found to be higher than those of unruptured aneurysms in the general population<sup>5, 94</sup>.

The risk of prevalence or rupture of intracranial aneurysms of patients with a history of one or more other family members suffering from SAH have been shown to depend on the number of affected relatives, increasing for one and particularly two or more relatives in comparison to the risk of sporadic cases<sup>151</sup>. Additionally, in familial aneurysms, some aneurysm characteristics such as location, size and the age at the rupture were shown to differ from sporadic aneurysms, being generally larger at time of rupture and more likely to be multiple. Thus, it has been suggested that familial aggregation may relate to genetic factors that determine defects of the arterial wall and interact with shared environmental factors that predispose to a relative weakness of the arterial wall<sup>150</sup>. However, no clear links to genetic determinants for aneurysms have been reported in the literature<sup>84</sup>, and the reported associations seem weaker in comparison to other factors. Moreover, based on a large population study of Nordic twins with a follow-up of 6 million person-years, heritability did not seem to be a determining factor for rupture. High incidence of SAH in a familial group has been most likely attributed to shared environmental risk factors rather than to a genetic origin<sup>21</sup>.

## Clinical Factors

Female gender, smoker and ADPKD are the major identified clinical risks factors for intracranial aneurysm formation. Smoking particularly has been shown to increase both, the formation of new aneurysms and the growth rate of preexisting ones<sup>20</sup>. Smoking is known to cause inflammation in the arterial walls, which in turns weakens and predisposes the wall for aneurysm formation. Most of the factors related to prevalence of aneurysms seem to relate or affect either the artery wall or the hemodynamic loads<sup>139</sup>.

It has been suggested that the increased female prevalence of cerebral aneurysms and SAH peaks in post-menopausal period, when there is a fall in estrogen levels. Changes in estrogen levels may have ramifications on vascular integrity, as it promotes the normal function of vascular wall<sup>60</sup>. It has also been suggested that anatomical and physiological factors such as

differences in vessel size and blood flow velocity result in higher hemodynamic forces acting on the vessel wall in females, increasing the risk of prevalence and rupture<sup>80</sup>.

Smoking seems to be an indisputable risk factor of rupture<sup>30, 59, 116, 121</sup>. It has been postulated that average SAH attack rate increases with age, and then it plateaus in older group, or even decreases after 50 years<sup>50</sup>. Hypertension is also considered among the major risk factors of rupture<sup>30, 121</sup>. It has been suggested that hypertension might be associated with both an increased aneurysm growth rate and inadequate wall repair, which may lead to rupture<sup>97</sup>. Another study proposed that smoking increased blood viscosity which in turn increased the WSS and OSI at sites where aneurysms usually develop<sup>124</sup>. However, this factor seems to be controversial. A case-control study of 163 new cases of SAH, reported that confirmed hypertension, based on target organ damage, was not an independent risk factor of SAH<sup>59</sup>.

A few studies have focused on trigger factors that could precipitate the rupture of intracranial aneurysms. One study found that there was no difference in the seasonal incidence of SAH, and that SAH occurs early in the morning while engaging in activities associated with Valsalva maneuvers<sup>85</sup>. Another study identified and quantified 8 out of 30 potential trigger factors in the period soon before subarachnoid hemorrhage<sup>130</sup>. In the case-crossover study, exposure to triggers is compared to the frequency of exposure. All triggers were related to sudden increase in blood pressure. The highest population-attributable risk factors were coffee consumption and vigorous physical exercise. Similarly, another study found that moderate to extreme physical exertion increased the risk of SAH during the 2-hour period after the physical activity<sup>4</sup>.

## Conclusions

The picture presented in Figure 1 summarizes the data and ideas presented in the literature reviewed in this article. Briefly, several factors induce biological processes in the wall that result in its progressive degeneration, remodeling, weakening and repair. The wall structure and hemodynamic loads determine the wall tension or stress which drives the geometric progression of the aneurysm. In turn, the aneurysm geometry, its size and shape, affects the flow pattern within the aneurysm sac. The hemodynamic environment together with the status of the aneurysm wall induce wall remodeling processes as well as thrombus formation and subsequent inflammation processes that affect the wall structure, thus closing the cycle. The peri-aneurysmal environment plays an important role when the aneurysm enters in contact with extra-vascular structures that constrain its shape thus influencing wall stresses and subsequent wall remodeling.

Other risk factors seem to indirectly influence this evolution cycle by either altering the hemodynamic loads or affecting the wall structure and cellular composition. Aneurysm location seems to be an important factor that influences the hemodynamics (e.g. through anatomic variants of the circle of Willis, arterial bifurcations, etc.), it also influences the wall structure (e.g. wall thickness at different locations, possible structural deficiencies at bifurcations, etc.), and determines whether the peri-aneurysmal environment is constraining or protective. Genetics and clinical factors seem to predispose the wall for aneurysm development or aggravate its chances of progression and rupture. Finally, rupture appears to occur when wall stress exceeds wall strength, typically precipitated by a trigger factor that suddenly increases the hemodynamic load (pressure).

Several studies have related hemodynamic and geometric variables to aneurysm formation, growth and rupture. However, to date, the results do not seem conclusive and in some cases seem to be in conflict. In our opinion, there are three main reasons: 1) the mechanisms of

aneurysm development are multi-factorial, therefore finding a single variable that determines if an aneurysm will rupture may be difficult; 2) there may be competing mechanisms simultaneously at play during the evolution of the aneurysms, for instance wall degeneration associated to abnormal NO production in response to high WSS, or wall degradation associated to inflammation from thrombus formation in regions of low WSS; and 3) the intrinsic limitations of the studies that have been carried out may prevent their direct comparison, generalization and interpretation.

Many studies have established correlations between geometric or hemodynamic variables and clinical events such as growth or rupture. The results of these studies have to be carefully interpreted. First, although correlation does not imply causation<sup>63</sup>, understanding the causes of aneurysm development and progression may help us understand the observed correlations. Therefore, correlation studies are important to constrain theories of aneurysm evolution, since these theories should be able to explain observations such as the ones summarized in this review. Secondly, univariate statistical analysis identifies variables related to rupture, for example, while multi-variate analysis retains independent variables with the strongest association to rupture and eliminates other dependent variables with weaker correlation to rupture. For instance, if max WSS and the area under low WSS (LSA) are not independent and one of them, say LSA, has a slight stronger correlation to rupture, it will be retained by the statistical model. However, this does not necessarily imply that the underlying mechanism is purely related to low WSS effects, it could actually be related to max WSS effects, or a combination of both. Therefore, it is important not only to identify variables connected to rupture (or other clinical events), but also to understand their inter-dependence.

The resolution of these apparent conflicts and identification of the mechanisms leading to wall degeneration and aneurysm progression will likely require multi-center studies based on a common approach and data selection criteria, uniform data analysis and modeling protocols, standardized variable definitions, and multiple populations<sup>22, 107, 128</sup>. Using longitudinal data of unruptured aneurysms, usually comprising small low risk aneurysms, is important to identify which of these aneurysms are likely to grow and subsequently rupture, and thus recommend their preventive treatment. On the other hand, the use of cross-sectional data (at a single time point) of ruptured and unruptured aneurysms is important to identify larger aneurysms that perhaps should be conservatively observed, thus preventing unnecessary interventions. Large multi-center samples are important to obtain statistically significant results valid across populations. Finally, the combination of clinical, imaging, epidemiological, biomechanical and biologic data is important to test hypotheses about the underlying mechanisms governing the natural history of cerebral aneurysms.

## Acknowledgments

This work was supported by the NIH grant #R01NS059063.

## References

1. Ahn S, Shin D, Tateshima S, Tanishita K, Vinuela F, Sinha S. Fluid-Induced Wall Shear Stress in Anthropomorphic Brain Aneurysm Models: Mr Phase-Contrast Study at 3 T. *J Magn Reson Imaging*. 2007; 25:1120–1130. [PubMed: 17520716]
2. Alnaes MS, Isaksen J, Mardal KA, Romner B, Morgan MK, Ingebrigtsen T. Computation of Hemodynamics in the Circle of Willis. *Stroke*. 2007; 38:2500–2505. [PubMed: 17673714]
3. Amenta PS, Yadla S, Campbell PG, Maltenfort MG, Dey S, Ghosh S, Ali MS, Jallo JI, Tjoumakaris SI, Gonzalez LF, Dumont AS, Rosenwasser RH, Jabbour PM. Analysis of Nonmodifiable Risk Factors for Intracranial Aneurysm Rupture in a Large, Retrospective Cohort. *Neurosurgery*. 2012; 70:693–699. discussion 99-701. [PubMed: 21904261]



4. Anderson C, Ni Mhurchu C, Scott D, Bennett D, Jamrozik K, Hankey G. Triggers of Subarachnoid Hemorrhage: Role of Physical Exertion, Smoking, and Alcohol in the Australasian Cooperative Research on Subarachnoid Hemorrhage Study (across). *Stroke*. 2003; 34:1771–1776. [PubMed: 12775890]
5. Audibert G, Bousquet S, Charpentier C, Devaux Y, Mertes PM. [Subarachnoid Haemorrhage: Epidemiology, Genomic, Clinical Presentation]. *Ann Fr Anesth Reanim*. 2007; 26:943–947. [PubMed: 17935939]
6. Baccin CE, Krings T, Alvarez H, Ozanne A, Lasjaunias P. Multiple Mirror-Like Intracranial Aneurysms. Report of a Case and Review of the Literature. *Acta Neurochir (Wien)*. 2006; 148:1091–1095. discussion 95. [PubMed: 16896548]
7. Baek H, Jayaraman MV, Karniadakis GE. Wall Shear Stress and Pressure Distribution on Aneurysms and Infundibulae in the Posterior Communicating Artery Bifurcation. *Ann Biomed Eng*. 2009; 37:2469–2487. [PubMed: 19757058]
8. Baharoglu MI, Schirmer CM, Hoit DA, Gao BL, Malek AM. Aneurysm Inflow-Angle as a Discriminant for Rupture in Sidewall Cerebral Aneurysms: Morphometric and Computational Fluid Dynamic Analysis. *Stroke*. 2010; 41:1423–1430. [PubMed: 20508183]
9. Beck J, Rohde S, Berkefeld J, Seifert V, Raabe A. Size and Location of Ruptured and Unruptured Intracranial Aneurysms Measured by 3-Dimensional Rotational Angiography. *Surg Neurol*. 2006; 65:18–25. discussion 25-7. [PubMed: 16378842]
10. Beck J, Rohde S, el Beltagy M, Zimmermann M, Berkefeld J, Seifert V, Raabe A. Difference in Configuration of Ruptured and Unruptured Intracranial Aneurysms Determined by Biplanar Digital Subtraction Angiography. *Acta Neurochir (Wien)*. 2003; 145:861–865. discussion 65. [PubMed: 14577007]
11. Boissonnat JD, Chaine R, Frey P, Malandain G, Salmon S, Saltel E, Thiriet M. From Arteriographies to Computational Flow in Saccular Aneurysms: The Inria Experience. *Med Image Anal*. 2005; 9:133–143. [PubMed: 15721229]
12. Boussel L, Rayz V, McCulloch C, Martin A, Acevedo-Bolton G, Lawton M, Higashida R, Smith WS, Young WL, Saloner D. Aneurysm Growth Occurs at Region of Low Wall Shear Stress: Patient-Specific Correlation of Hemodynamics and Growth in a Longitudinal Study. *Stroke*. 2008; 39:2997–3002. [PubMed: 18688012]
13. Campos C, Churojana A, Rodesch G, Alvarez H, Lasjaunias P. Multiple Intracranial Arterial Aneurysms: A Congenital Metameric Disease? Review of 113 Consecutive Patients with 280 Aa. *Interv Neuroradiol*. 1998; 4:293–299. [PubMed: 20673425]
14. Carter BS, Sheth S, Chang E, Sethl M, Ogilvy CS. Epidemiology of the Size Distribution of Intracranial Bifurcation Aneurysms: Smaller Size of Distal Aneurysms and Increasing Size of Unruptured Aneurysms with Age. *Neurosurgery*. 2006; 58:217–223. discussion 17-23. [PubMed: 16462474]
15. Casimiro MV, McEvoy AW, Watkins LD, Kitchen ND. A Comparison of Risk Factors in the Etiology of Mirror and Nonmirror Multiple Intracranial Aneurysms. *Surg Neurol*. 2004; 61:541–545. [PubMed: 15165792]
16. Castro M, Putman CM, Cebal JR. Patient-Specific Computational Modeling of Cerebral Aneurysms with Multiple Avenues of Flow from 3d Rotational Angiography Images. *Acad Radiol*. 2006; 13:811–821. [PubMed: 16777554]
17. Castro MA, Putman CM, Cebal JR. Patient-Specific Computational Fluid Dynamics Modeling of Anterior Communicating Artery Aneurysms: A Study of the Sensitivity of Intra-Aneurysmal Flow Patterns to Flow Conditions in the Carotid Arteries. *AJNR Am J Neuroradiol*. 2006; 27:2061–2068. [PubMed: 17110667]
18. Castro MA, Putman CM, Sheridan MJ, Cebal JR. Hemodynamic Patterns of Anterior Communicating Artery Aneurysms: A Possible Association with Rupture. *AJNR Am J Neuroradiol*. 2009; 30:297–302. [PubMed: 19131411]
19. Castro M, Putman C, Radaelli A, Frangi A, Cebal J. Hemodynamics and Rupture of Terminal Cerebral Aneurysms. *Acad Radiol*. 2009; 16:1201–1207. [PubMed: 19553143]

20. Cebal JR, Castro MA, Burgess JE, Pergolizzi RS, Sheridan MJ, Putman CM. Characterization of Cerebral Aneurysms for Assessing Risk of Rupture by Using Patient-Specific Computational Hemodynamics Models. *AJNR Am J Neuroradiol.* 2005; 26:2550–2559. [PubMed: 16286400]
21. Cebal JR, Hendrickson S, Putman CM. Hemodynamics in a Lethal Basilar Artery Aneurysm Just before Its Rupture. *AJNR Am J Neuroradiol.* 2009; 30:95–98. [PubMed: 18818279]
22. Cebal JR, Meng H. Counterpoint: Realizing the Clinical Utility of Computational Fluid Dynamics--Closing the Gap. *AJNR Am J Neuroradiol.* 2012; 33:396–398. [PubMed: 22282452]
23. Cebal JR, Mut F, Weir J, Putman C. Quantitative Characterization of the Hemodynamic Environment in Ruptured and Unruptured Brain Aneurysms. *AJNR Am J Neuroradiol.* 2011; 32:145–151. [PubMed: 21127144]
24. Cebal JR, Mut F, Weir J, Putman CM. Association of Hemodynamic Characteristics and Cerebral Aneurysm Rupture. *AJNR Am J Neuroradiol.* 2011; 32:264–270. [PubMed: 21051508]
25. Cebal JR, Sheridan M, Putman CM. Hemodynamics and Bleb Formation in Intracranial Aneurysms. *AJNR Am J Neuroradiol.* 2010; 31:304–310. [PubMed: 19797790]
26. Chien A, Castro MA, Tateshima S, Sayre J, Cebal J, Vinuela F. Quantitative Hemodynamic Analysis of Brain Aneurysms at Different Locations. *AJNR Am J Neuroradiol.* 2009; 30:1507–1512. [PubMed: 19406766]
27. Chien A, Sayre J, Vinuela F. Comparative Morphological Analysis of the Geometry of Ruptured and Unruptured Aneurysms. *Neurosurgery.* 2011; 69:349–356. [PubMed: 21415785]
28. Chien A, Tateshima S, Castro M, Sayre J, Cebal J, Vinuela F. Patient-Specific Flow Analysis of Brain Aneurysms at a Single Location: Comparison of Hemodynamic Characteristics in Small Aneurysms. *Med Biol Eng Comput.* 2008; 46:1113–1120. [PubMed: 18931868]
29. Chien A, Tateshima S, Sayre J, Castro M, Cebal J, Vinuela F. Patient-Specific Hemodynamic Analysis of Small Internal Carotid Artery-Ophthalmic Artery Aneurysms. *Surg Neurol.* 2009; 72:444–450. discussion 50. [PubMed: 19329152]
30. Chmaysani M, Rebeiz JG, Rebeiz TJ, Batjer HH, Bendok BR. Relationship of Growth to Aneurysm Rupture in Asymptomatic Aneurysms  $\leq 7$  Mm: A Systematic Analysis of the Literature. *Neurosurgery.* 2011; 68:1164–1171. discussion 71. [PubMed: 21307791]
31. Choi IS, David C. Giant Intracranial Aneurysms: Development, Clinical Presentation and Treatment. *Eur J Radiol.* 2003; 46:178–194. [PubMed: 12758113]
32. Clarke G, Mendelow AD, Mitchell P. Predicting the Risk of Rupture of Intracranial Aneurysms Based on Anatomical Location. *Acta Neurochir (Wien).* 2005; 147:259–263. discussion 63. [PubMed: 15662565]
33. Clarke M. Systematic Review of Reviews of Risk Factors for Intracranial Aneurysms. *Neuroradiology.* 2008; 50:653–664. [PubMed: 18560819]
34. Costalat V, Sanchez M, Ambard D, Thines L, Lonjon N, Nicoud F, Brunel H, Lejeune JP, Dufour H, Bouillot P, Lhaldky JP, Kouri K, Segnarbieux F, Maurage CA, Lobotesis K, Villa-Uriol MC, Zhang C, Frangi AF, Mercier G, Bonafe A, Sarry L, Jourdan F. Biomechanical Wall 30 Properties of Human Intracranial Aneurysms Resected Following Surgical Clipping (Irras Project). *J Biomech.* 2011; 44:2685–2691. [PubMed: 21924427]
35. Dashti R, Hernesniemi J, Lehto H, Niemela M, Lehecka M, Rinne J, Porras M, Ronkainen A, Phornsuwannapha S, Koivisto T, Jaaskelainen JE. Microneurosurgical Management of Proximal Anterior Cerebral Artery Aneurysms. *Surg Neurol.* 2007; 68:366–377. [PubMed: 17905060]
36. de Rooij NK, Velthuis BK, Algra A, Rinkel GJ. Configuration of the Circle of Willis, Direction of Flow, and Shape of the Aneurysm as Risk Factors for Rupture of Intracranial Aneurysms. *J Neurol.* 2009; 256:45–50. [PubMed: 19221852]
37. Dhar S, Tremmel M, Mocco J, Kim M, Yamamoto J, Siddiqui AH, Hopkins LN, Meng H. Morphology Parameters for Intracranial Aneurysm Rupture Risk Assessment. *Neurosurgery.* 2008; 63:185–196. discussion 96-7. [PubMed: 18797347]
38. Foutrakis GN, Yonas H, Sclabassi RJ. Saccular Aneurysm Formation in Curved and Bifurcating Arteries. *AJNR Am J Neuroradiol.* 1999; 20:1309–1317. [PubMed: 10472991]
39. Frosen J, Piippo A, Paetau A, Kangasniemi M, Niemela M, Hernesniemi J, Jaaskelainen J. Remodeling of Saccular Cerebral Artery Aneurysm Wall Is Associated with Rupture: Histological

- Analysis of 24 Unruptured and 42 Ruptured Cases. *Stroke*. 2004; 35:2287–2293. [PubMed: 15322297]
40. Frosen J, Tulamo R, Paetau A, Laaksamo E, Korja M, Laakso A, Niemela M, Hernesniemi J. Saccular Intracranial Aneurysm: Pathology and Mechanisms. *Acta Neuropathol*. 2012; 123:773–786. [PubMed: 22249619]
  41. Hamada J, Morioka M, Yano S, Todaka T, Kai Y, Kuratsu J. Clinical Features of Aneurysms of the Posterior Cerebral Artery: A 15-Year Experience with 21 Cases. *Neurosurgery*. 2005; 56:662–670. discussion 62-70. [PubMed: 15792504]
  42. Hans FJ, Krings T, Reinges MH, Mull M. Spontaneous Regression of Two Supraophthalmic Internal Cerebral Artery Aneurysms Following Flow Pattern Alteration. *Neuroradiology*. 2004; 46:469–473. [PubMed: 15150678]
  43. Hashimoto N, Handa H, Nagata I, Hazama F. Animal Model of Cerebral Aneurysms: Pathology and Pathogenesis of Induced Cerebral Aneurysms in Rats. *Neurol Res*. 1984; 6:33–40. [PubMed: 6147777]
  44. Hassan T, Hassan AA, Ahmed YM. Influence of Parent Vessel Dominancy on Fluid Dynamics of Anterior Communicating Artery Aneurysms. *Acta Neurochir (Wien)*. 2011; 153:305–310. [PubMed: 20924768]
  45. Hassan T, Timofeev EV, Saito T, Shimizu H, Ezura M, Matsumoto Y, Takayama K, Tominaga T, Takahashi A. A Proposed Parent Vessel Geometry-Based Categorization of Saccular 31 Intracranial Aneurysms: Computational Flow Dynamics Analysis of the Risk Factors for Lesion Rupture. *J Neurosurg*. 2005; 103:662–680. [PubMed: 16266049]
  46. Hayakawa M, Maeda S, Sadato A, Tanaka T, Kaito T, Hattori N, Ganaha T, Moriya S, Katada K, Murayama K, Kato Y, Hirose Y. Detection of Pulsation in Ruptured and Unruptured Cerebral Aneurysms by Electrocardiographically Gated 3-Dimensional Computed Tomographic Angiography with a 320-Row Area Detector Computed Tomography and Evaluation of Its Clinical Usefulness. *Neurosurgery*. 2011; 69:843–851. discussion 51. [PubMed: 21623246]
  47. He W, Hauptman J, Pasupuleti L, Setton A, Farrow MG, Kasper L, Karimi R, Gandhi CD, Catrambone JE, Prestigiacomo CJ. True Posterior Communicating Artery Aneurysms: Are They More Prone to Rupture? A Biomorphometric Analysis. *J Neurosurg*. 2010; 112:611–615. [PubMed: 19747044]
  48. Higa T, Ujiie H, Kato K, Kamiyama H, Hori T. Basilar Artery Trunk Saccular Aneurysms: Morphological Characteristics and Management. *Neurosurg Rev*. 2009; 32:181–191. discussion 91. [PubMed: 18791752]
  49. Hoh BL, Siström CL, Firment CS, Fautheree GL, Velat GJ, Whiting JH, Reavey-Cantwell JF, Lewis SB. Bottleneck Factor and Height-Width Ratio: Association with Ruptured Aneurysms in Patients with Multiple Cerebral Aneurysms. *Neurosurgery*. 2007; 61:716–722. discussion 22-3. [PubMed: 17986932]
  50. Imbesi SG, Kerber CW. Analysis of Slipstream Flow in Two Ruptured Intracranial Cerebral Aneurysms. *AJNR Am J Neuroradiol*. 1999; 20:1703–1705. [PubMed: 10543644]
  51. Isaksen JG, Bazilevs Y, Kvamsdal T, Zhang Y, Kaspersen JH, Waterloo K, Romner B, Ingebrigtsen T. Determination of Wall Tension in Cerebral Artery Aneurysms by Numerical Simulation. *Stroke*. 2008; 39:3172–3178. [PubMed: 18818402]
  52. Ishikawa T, Nakayama N, Yoshimoto T, Aoki T, Terasaka S, Nomura M, Takahashi A, Kuroda S, Iwasaki Y. How Does Spontaneous Hemostasis Occur in Ruptured Cerebral Aneurysms? Preliminary Investigation on 247 Clipping Surgeries. *Surg Neurol*. 2006; 66:269–275. discussion 75-6. [PubMed: 16935633]
  53. Jayakrishnan VK, Rodesch G, Alvarez H, Lasjaunias P. A Case of Multiple Intracranial Aneurysms with Unruptured Associated Aneurysms and Newly Developed Ruptured Aneurysm. *Interv Neuroradiol*. 2001; 7:259–262. [PubMed: 20663357]
  54. Jeong YG, Jung YT, Kim MS, Eun CK, Jang SH. Size and Location of Ruptured Intracranial Aneurysms. *J Korean Neurosurg Soc*. 2009; 45:11–15. [PubMed: 19242565]
  55. Joo SP, Kim TS, Choi JW, Lee JW, Kim YW, Moon KW, Kim JH, Kim SH. Characteristics and Management of Ruptured Distal Middle Cerebral Artery Aneurysms. *Acta Neurochir (Wien)*. 2007; 149:661–667. [PubMed: 17541490]

56. Joo SW, Lee SW, Noh SW, Jeong YW, Kim MW, Jeong YT. What Is the Significance of a Large Number of Ruptured Aneurysms Smaller Than 7 Mm in Diameter? *J Korean Neurosurg Soc.* 2009; 45:85–89. [PubMed: 19274117]
57. Jou LD, Lee DH, Mawad ME. Cross-Flow at the Anterior Communicating Artery and Its Implication in Cerebral Aneurysm Formation. *J Biomech.* 2010; 43:2189–2195. [PubMed: 20447636]
58. Jou LD, Lee DH, Morsi H, Mawad ME. Wall Shear Stress on Ruptured and Unruptured Intracranial Aneurysms at the Internal Carotid Artery. *AJNR Am J Neuroradiol.* 2008; 29:1761–1767. [PubMed: 18599576]
59. Jou LD, Mawad ME. Timing and Size of Flow Impingement in a Giant Intracranial Aneurysm at the Internal Carotid Artery. *Med Biol Eng Comput.* 2011; 49:891–899. [PubMed: 21210303]
60. Jou LD, Wong G, Dispensa B, Lawton MW, Higashida RW, Young WW, Saloner D. Correlation between Luminal Geometry Changes and Hemodynamics in Fusiform Intracranial Aneurysms. *AJNR Am J Neuroradiol.* 2005; 26:2357–2363. [PubMed: 16219845]
61. Juvela S, Poussa K, Porras M. Factors Affecting Formation and Growth of Intracranial Aneurysms: A Long-Term Follow-up Study. *Stroke.* 2001; 32:485–491. [PubMed: 11157187]
62. Kadasi LM, Dent WW, Malek AM. Cerebral Aneurysm Wall Thickness Analysis Using Intraoperative Microscopy: Effect of Size and Gender on Thin Translucent Regions. *J Neurointerv Surg.* 2012
63. Kallmes DF. Point: Cfd--Computational Fluid Dynamics or Confounding Factor Dissemination. *AJNR Am J Neuroradiol.* 2012; 33:395–396. [PubMed: 22268081]
64. Kasuya H, Shimizu T, Nakaya K, Sasahara A, Hori T, Takakura K. Angeles between A1 and A2 Segments of the Anterior Cerebral Artery Visualized by Three-Dimensional Computed Tomographic Angiography and Association of Anterior Communicating Artery Aneurysms. *Neurosurgery.* 1999; 45:89–93. discussion 93-4. [PubMed: 10414570]
65. Kataoka K, Taneda M, Asai T, Kinoshita A, Ito M, Kuroda R. Structural Fragility and Inflammatory Response of Ruptured Cerebral Aneurysms. A Comparative Study between Ruptured and Unruptured Cerebral Aneurysms. *Stroke.* 1999; 30:1396–1401. [PubMed: 10390313]
66. Kupersmith MJ, Stiebel-Kalish H, Huna-Baron R, Setton A, Niimi Y, Langer D, Berenstein A. Cavernous Carotid Aneurysms Rarely Cause Subarachnoid Hemorrhage or Major Neurologic Morbidity. *J Stroke Cerebrovasc Dis.* 2002; 11:9–14. [PubMed: 17903849]
67. Kwak R, Niizuma H, Suzuki J. Hemodynamics in the Anterior Part of the Circle of Willis in Patients with Intracranial Aneurysms: A Study of Cerebral Angiography. *Tohoku J Exp Med.* 1980; 132:69–73. [PubMed: 7209970]
68. Kwak R, Ohi T, Niizuma H, Suzuki J. [Relationship between the Afferent Artery and the Site of Neck of Anterior Communicating Artery Aneurysm, and Hemodynamics in the Anterior Part of the Circle of Willis (Author's Transl)]. *No Shinkei Geka.* 1978; 6:1159–1163. [PubMed: 732933]
69. Kyriacou SK, Humphrey JD. Influence of Size, Shape and Properties on the Mechanics of Axisymmetric Saccular Aneurysms. *J Biomech.* 1996; 29:1015–1022. [PubMed: 8817368]
70. Lai HP, Cheng KW, Yu SW, Au Yeung KW, Cheung YW, Chan CW, Poon WW, Lui WM. Size, Location, and Multiplicity of Ruptured Intracranial Aneurysms in the Hong Kong Chinese Population with Subarachnoid Haemorrhage. *Hong Kong Med J.* 2009; 15:262–266. [PubMed: 19652232]
71. Lauric A, Miller EL, Baharoglu MI, Malek AM. Rupture Status Discrimination in Intracranial Aneurysms Using the Centroid-Radii Model. *IEEE Trans Biomed Eng.* 2011; 58:2895–2903. [PubMed: 21775251]
72. Lauric A, Baharoglu MW, Gao BW, Malek AM. Incremental Contribution of Size Ratio as a Discriminant for Rupture Status in Cerebral Aneurysms: Comparison with Size, Height, and Vessel Diameter. *Neurosurgery.* 2012; 70:944–951. discussion 51-2. [PubMed: 21997542]
73. Lauric A, Baharoglu MW, Malek AM. Ruptured Status Discrimination Performance of Aspect Ratio, Height/Width, and Bottleneck Factor Is Highly Dependent on Aneurysm Sizing Methodology. *Neurosurgery.* 2012; 71:38–46. [PubMed: 22353797]

74. Lauric A, Miller EW, Baharoglu MW, Malek AM. 3d Shape Analysis of Intracranial Aneurysms Using the Writhe Number as a Discriminant for Rupture. *Ann Biomed Eng.* 2011; 39:1457–1469. [PubMed: 21225345]
75. Lazzaro MA, Ouyang B, Chen M. The Role of Circle of Willis Anomalies in Cerebral Aneurysm Rupture. *J Neurointerv Surg.* 2012; 4:22–26. [PubMed: 21990452]
76. Lee JM, Joo SW, Kim TW, Go EW, Choi HW, Seo BR. Surgical Management of Anterior Cerebral Artery Aneurysms of the Proximal (A1) Segment. *World Neurosurg.* 2010; 74:478–482. [PubMed: 21492598]
77. Lee JY, Kim MW, Cho BW, Park SH, Oh SM. Surgical Experience of the Ruptured Distal Anterior Cerebral Artery Aneurysms. *J Korean Neurosurg Soc.* 2007; 42:281–285. [PubMed: 19096557]
78. Lehecka M, Dashti R, Hernesniemi J, Niemela M, Koivisto T, Ronkainen A, Rinne J, Jaaskelainen J. Microneurosurgical Management of Aneurysms at the A2 Segment of Anterior Cerebral Artery (Proximal Pericallosal Artery) and Its Frontobasal Branches. *Surg Neurol.* 2008; 70:232–246. discussion 46. [PubMed: 18486199]
79. Lehecka M, Dashti R, Laakso A, van Popta JW, Romani R, Navratil O, Kivipelto L, Kivisaari R, Foroughi M, Kokuzawa J, Lehto H, Niemela M, Rinne J, Ronkainen A, Koivisto T, Jaaskelainen JW, Hernesniemi J. Microneurosurgical Management of Anterior Choroid Artery Aneurysms. *World Neurosurg.* 2010; 73:486–499. [PubMed: 20920932]
80. Lindekleiv HM, Valen-Sendstad K, Morgan MW, Mardal KW, Faulder K, Magnus JH, Waterloo K, Romner B, Ingebrigtsen T. Sex Differences in Intracranial Arterial Bifurcations. *Gend Med.* 2010; 7:149–155. [PubMed: 20435277]
81. Lu G, Huang L, Zhang XW, Wang SW, Hong Y, Hu Z, Geng DY. Influence of Hemodynamic Factors on Rupture of Intracranial Aneurysms: Patient-Specific 3d Mirror Aneurysms Model Computational Fluid Dynamics Simulation. *AJNR Am J Neuroradiol.* 2011; 32:1255–1261. [PubMed: 21757526]
82. Ma B, Harbaugh RW, Raghavan ML. Three-Dimensional Geometrical Characterization of Cerebral Aneurysms. *Ann Biomed Eng.* 2004; 32:264–273. [PubMed: 15008374]
83. MacDonald, RL.; Weir, B. Pathophysiology and Clinical Evaluation of Subarachnoid Hemorrhage. In: Youmans, JR., editor. *Neurological Survey.* Philadelphia, PA: W.B. Saunders Company; 1996.
84. Mantha A, Karmonik C, Benndorf G, Strother C, Metcalfe R. Hemodynamics in a Cerebral Artery before and after the Formation of an Aneurysm. *AJNR Am J Neuroradiol.* 2006; 27:1113–1118. [PubMed: 16687554]
85. Matsuda M, Watanabe K, Saito A, Matsumura K, Ichikawa M. Circumstances, Activities, and Events Precipitating Aneurysmal Subarachnoid Hemorrhage. *J Stroke Cerebrovasc Dis.* 2007; 16:25–29. [PubMed: 17689388]
86. Meng H, Feng Y, Woodward SH, Bendok BW, Hanel RW, Guterman LW, Hopkins LN. Mathematical Model of the Rupture Mechanism of Intracranial Saccular Aneurysms through Daughter Aneurysm Formation and Growth. *Neurol Res.* 2005; 27:459–465. [PubMed: 15978170]
87. Metaxa E, Tremmel M, Natarajan SW, Xiang J, Paluch RA, Mandelbaum M, Siddiqui AH, Kolega J, Mocco J, Meng H. Characterization of Critical Hemodynamics Contributing to Aneurysmal Remodeling at the Basilar Terminus in a Rabbit Model. *Stroke.* 2010; 41:1774–1782. [PubMed: 20595660]
88. Millan RD, Dempere-Marco L, Pozo JM, Cebal JR, Frangi AF. Morphological Characterization of Intracranial Aneurysms Using 3-D Moment Invariants. *IEEE Trans Med Imaging.* 2007; 26:1270–1282. [PubMed: 17896598]
89. Murray CD. The Physiological Principle of Minimum Work: I. The Vascular System and the Cost of Blood Volume. *Proc Natl Acad Sci U S A.* 1926; 12:207–214. [PubMed: 16576980]
90. Murray CD. The Physiological Principle of Minimum Work Applied to the Angle of Branching of Arteries. *J Gen Physiol.* 1926; 9:835–841. [PubMed: 19872299]
91. Nader-Sepahi A, Casimiro M, Sen J, Kitchen ND. Is Aspect Ratio a Reliable Predictor of Intracranial Aneurysm Rupture? *Neurosurgery.* 2004; 54:1343–1347. discussion 47-8. [PubMed: 15157290]

92. Nixon AM, Gunel M, Sumpio BE. The Critical Role of Hemodynamics in the Development of Cerebral Vascular Disease. *J Neurosurg.* 2010; 112:1240–1253. [PubMed: 19943737]
93. Nystrom SH. On Factors Related to Growth and Rupture of Intracranial Aneurysms. *Acta Neuropathol.* 1970; 16:64–72. [PubMed: 5456388]
94. Oh YS, Shon YM, Kim BS, Cho AH. Long-Term Follow-up of Incidental Intracranial Aneurysms in Patients with Acute Ischemic Stroke. *J Stroke Cerebrovasc Dis.* 2011
95. Ohashi Y, Horikoshi T, Sugita M, Yagishita T, Nukui H. Size of Cerebral Aneurysms and Related Factors in Patients with Subarachnoid Hemorrhage. *Surg Neurol.* 2004; 61:239–245. discussion 45-7. [PubMed: 14984993]
96. Ohshima T, Miyachi S, Hattori K, Takahashi I, Ishii K, Izumi T, Yoshida J. Risk of Aneurysmal Rupture: The Importance of Neck Orifice Positioning-Assessment Using Computational Flow Simulation. *Neurosurgery.* 2008; 62:767–773. discussion 73-5. [PubMed: 18496182]
97. Park DH, Kang SH, Lee JB, Lim DJ, Kwon TH, Chung YG, Lee HK. Angiographic Features, Surgical Management and Outcomes of Proximal Middle Cerebral Artery Aneurysms. *Clin Neurol Neurosurg.* 2008; 110:544–551. [PubMed: 18367320]
98. Park JK, Lee CS, Sim KB, Huh JS, Park JC. Imaging of the Walls of Saccular Cerebral Aneurysms with Double Inversion Recovery Black-Blood Sequence. *J Magn Reson Imaging.* 2009; 30:1179–1183. [PubMed: 19856452]
99. Peluso JP, van Rooij WJ, Sluzewski M, Beute GN, Majoie CB. Posterior Inferior Cerebellar Artery Aneurysms: Incidence, Clinical Presentation, and Outcome of Endovascular Treatment. *AJNR Am J Neuroradiol.* 2008; 29:86–90. [PubMed: 17928380]
100. Penn DL, Komotar RJ, Sander Connolly E. Hemodynamic Mechanisms Underlying Cerebral Aneurysm Pathogenesis. *J Clin Neurosci.* 2011; 18:1435–1438. [PubMed: 21917457]
101. Prestigiacomo CJ, He W, Catrambone J, Chung S, Kasper L, Pasupuleti L, Mittal N. Predicting Aneurysm Rupture Probabilities through the Application of a Computed Tomography Angiography-Derived Binary Logistic Regression Model. *J Neurosurg.* 2009; 110:1–6. [PubMed: 18928360]
102. Qi W, Wang S, Zhao YL, Yang HB, Zhao JZ. Clinical Characteristics and Surgical Treatment of Patients with Giant Intracranial Aneurysms. *Chin Med J (Engl).* 2008; 121:1085–1088. [PubMed: 18706222]
103. Qian Y, Takao H, Umezu M, Murayama Y. Risk Analysis of Unruptured Aneurysms Using Computational Fluid Dynamics Technology: Preliminary Results. *AJNR Am J Neuroradiol.* 2011; 32:1948–1955. [PubMed: 21903914]
104. Quintero-Oliveros ST, Ballesteros-Acuna LE, Ayala-Pimentel JO, Forero-Porras PL. Morphological Characteristics of Cerebral Aneurysm of Willis' Circle: A Direct Anatomical Study. *Neurocirugia (Astur).* 2009; 20:110–116. [PubMed: 19448955]
105. Rahman M, Smietana J, Hauck E, Hoh B, Hopkins N, Siddiqui A, Levy EI, Meng H, Mocco J. Size Ratio Correlates with Intracranial Aneurysm Rupture Status: A Prospective Study. *Stroke.* 2010; 41:916–920. [PubMed: 20378866]
106. Rinkel GJ, Djibuti M, Algra A, van Gijn J. Prevalence and Risk of Rupture of Intracranial Aneurysms: A Systematic Review. *Stroke.* 1998; 29:251–256. [PubMed: 9445359]
107. Robertson AM, Watton PN. Computational Fluid Dynamics in Aneurysm Research: Critical Reflections, Future Directions. *AJNR Am J Neuroradiol.* 2012; 33:992–995. [PubMed: 22653325]
108. Ryu CW, Kwon OK, Koh JS, Kim EJ. Analysis of Aneurysm Rupture in Relation to the Geometric Indices: Aspect Ratio, Volume, and Volume-to-Neck Ratio. *Neuroradiology.* 2011; 53:883–889. [PubMed: 21107548]
109. Sakamoto S, Ohba S, Shibukawa M, Kiura Y, Okazaki T, Arita K, Kurisu K. Characteristics of Aneurysms of the Internal Carotid Artery Bifurcation. *Acta Neurochir (Wien).* 2006; 148:139–143. discussion 43. [PubMed: 16322905]
110. San Millan Ruiz D, Tokunaga K, Dehdashti AR, Sugiu K, Delavelle J, Rufenacht DA. Is the Rupture of Cerebral Berry Aneurysms Influenced by the Perianeurysmal Environment? *Acta Neurochir Suppl.* 2002; 82:31–34. [PubMed: 12378987]

111. San Millan Ruiz D, Yilmaz H, Dehdashti AR, Alimenti A, de Tribolet N, Rufenacht DA. The Perianeurysmal Environment: Influence on Saccular Aneurysm Shape and Rupture. *AJNR Am J Neuroradiol.* 2006; 27:504–512. [PubMed: 16551985]
112. Sato K, Yoshimoto Y. Risk Profile of Intracranial Aneurysms: Rupture Rate Is Not Constant after Formation. *Stroke.* 2011; 42:3376–3381. [PubMed: 21980206]
113. Satoh T, Omi M, Ohsako C, Katsumata A, Yoshimoto Y, Tsuchimoto S, Onoda K, Tokunaga K, Sugi K, Date I. Influence of Perianeurysmal Environment on the Deformation and Bleb Formation of the Unruptured Cerebral Aneurysm: Assessment with Fusion Imaging of 3d Mr Cisternography and 3d Mr Angiography. *AJNR Am J Neuroradiol.* 2005; 26:2010–2018. [PubMed: 16155151]
114. Seoane ER, Tedeschi H, de Oliveira E, Siqueira MG, Calderon GA, Rhoton AL Jr. Management Strategies for Posterior Cerebral Artery Aneurysms: A Proposed New Surgical Classification. *Acta Neurochir (Wien).* 1997; 139:325–331. [PubMed: 9202772]
115. Seshaiyer P, Humphrey JD. On the Potentially Protective Role of Contact Constraints on Saccular Aneurysms. *J Biomech.* 2001; 34:607–612. [PubMed: 11311701]
116. Sforza DM, Putman C, Cebal J. Computational Fluid Dynamics (Cfd) in Brain Aneurysms. *Int J Numer Meth Biomed Engng.* 2012; 28:801–808.
117. Sforza DM, Putman CM, Cebal JR. Hemodynamics of Cerebral Aneurysms. *Annu Rev Fluid Mech.* 2009; 41:91–107. [PubMed: 19784385]
118. Sforza DM, Putman CM, Scrivano E, Lylyk P, Cebal JR. Blood-Flow Characteristics in a Terminal Basilar Tip Aneurysm Prior to Its Fatal Rupture. *AJNR Am J Neuroradiol.* 2010; 31:1127–1131. [PubMed: 20150312]
119. Sforza DM, Putman CM, Tateshima S, Vinuela F, Cebal JR. Effects of Perianeurysmal Environment During the Growth of Cerebral Aneurysms: A Case Study. *AJNR Am J Neuroradiol.* 2012; 33:1115–1120. [PubMed: 22300939]
120. Sforza, DM.; Putman, C.; Tateshima, S.; Vinuela, F.; Cebal, J. Summer Bioengineering Conference (SBC2012). Fajardo: Puerto Rico; 2012. Hemodynamic Characteristics of Growing and Stable Aneurysms', in.
121. Shimogonya Y, Ishikawa T, Imai Y, Matsuki N, Yamaguchi T. Can Temporal Fluctuation in Spatial Wall Shear Stress Gradient Initiate a Cerebral Aneurysm? A Proposed Novel Hemodynamic Index, the Gradient Oscillatory Number (Gon). *J Biomech.* 2009; 42:550–554. [PubMed: 19195658]
122. Shojima M, Nemoto S, Morita A, Oshima M, Watanabe E, Saito N. Role of Shear Stress in the Blister Formation of Cerebral Aneurysms. *Neurosurgery.* 2010; 67:1268–1274. discussion 74-5. [PubMed: 20948401]
123. Shojima M, Oshima M, Takagi K, Torii R, Hayakawa M, Katada K, Morita A, Kirino T. Magnitude and Role of Wall Shear Stress on Cerebral Aneurysm: Computational Fluid Dynamic Study of 20 Middle Cerebral Artery Aneurysms. *Stroke.* 2004; 35:2500–2505. [PubMed: 15514200]
124. Singh PK, Marzo A, Howard B, Rufenacht DW, Bijlenga P, Frangi AW, Lawford PW, Coley SW, Hose DW, Patel UJ. Effects of Smoking and Hypertension on Wall Shear Stress and Oscillatory Shear Index at the Site of Intracranial Aneurysm Formation. *Clin Neurol Neurosurg.* 2010; 112:306–313. [PubMed: 20096503]
125. Songsaeng D, Geibprasert S, Willinsky R, Tymianski M, TerBrugge KW, Krings T. Impact of Anatomical Variations of the Circle of Willis on the Incidence of Aneurysms and Their Recurrence Rate Following Endovascular Treatment. *Clin Radiol.* 2010; 65:895–901. [PubMed: 20933644]
126. Stehbens WE. Familial Intracranial Aneurysms: An Autopsy Study. *Neurosurgery.* 1998; 43:1258–1259. [PubMed: 9802874]
127. Stehbens WE. Etiology of Intracranial Berry Aneurysms. *J Neurosurg.* 1989; 70:823–831. [PubMed: 2654334]
128. Strother CM. Intracranial Aneurysms, Cancer, X-Rays and Computational Fluid Dynamics. *AJNR American Journal of Neuroradiology.* 2012

129. Sugiu K, Jean B, San Millan Ruiz D, Martin JW, Delavelle J, Rufenacht DA. Influence of the Perianeurysmal Environment on Rupture of Cerebral Aneurysms. Preliminary Observation. *Interv Neuroradiol.* 2000; 6(Suppl 1):65–70. [PubMed: 20667223]
130. Sugiyama SI, Meng H, Funamoto K, Inoue T, Fujimura M, Nakayama T, Omodaka S, Shimizu H, Takahashi A, Tominaga T. Hemodynamic Analysis of Growing Intracranial Aneurysms Arising from a Posterior Inferior Cerebellar Artery. *World Neurosurg.* 2011
131. Szikora I, Paal G, Ugron A, Naszstanovics F, Marosfoi M, Berentei Z, Kulcsar Z, Lee W, Bojtar I, Nyary I. Impact of Aneurysmal Geometry on Intraaneurysmal Flow: A Computerized Flow Simulation Study. *Neuroradiology.* 2008; 50:411–421. [PubMed: 18180916]
132. Takao H, Murayama Y, Otsuka S, Qian Y, Mohamed A, Masuda S, Yamamoto M, Abe T. Hemodynamic Differences between Unruptured and Ruptured Intracranial Aneurysms During Observation. *Stroke.* 2012; 43:1436–1439. [PubMed: 22363053]
133. Takeuchi S, Karino T. Flow Patterns and Distributions of Fluid Velocity and Wall Shear Stress in the Human Internal Carotid and Middle Cerebral Arteries. *World Neurosurg.* 2010; 73:174–185. discussion e27. [PubMed: 20860955]
134. Tateshima S, Murayama Y, Villablanca JW, Morino T, Nomura K, Tanishita K, Vinuela F. In Vitro Measurement of Fluid-Induced Wall Shear Stress in Unruptured Cerebral Aneurysms Harboring Blebs. *Stroke.* 2003; 34:187–192. [PubMed: 12511772]
135. Tremmel M, Dhar S, Levy EW, Mocco J, Meng H. Influence of Intracranial Aneurysm-to-Parent Vessel Size Ratio on Hemodynamics and Implication for Rupture: Results from a Virtual Experimental Study. *Neurosurgery.* 2009; 64:622–630. discussion 30-1. [PubMed: 19349824]
136. Ujii H, Liepsch DW, Goetz M, Yamaguchi R, Yonetani H, Takakura K. Hemodynamic Study of the Anterior Communicating Artery. *Stroke.* 1996; 27:2086–2093. discussion 94. [PubMed: 8898821]
137. Ujii H, Tamano Y, Sasaki K, Hori T. Is the Aspect Ratio a Reliable Index for Predicting the Rupture of a Saccular Aneurysm? *Neurosurgery.* 2001; 48:495–502. discussion 02-3. [PubMed: 11270538]
138. Valen-Sendstad K, Mardal KW, Reif BW, Langtangen HP. Direct Numerical Simulation of Transitional Flow in a Patient-Specific Intracranial Aneurysm. *J Biomech.* 2011; 44:2826–2832. [PubMed: 21924724]
139. Valencia A, Morales H, Rivera R, Bravo E, Galvez M. Blood Flow Dynamics in Patient-Specific Cerebral Aneurysm Models: The Relationship between Wall Shear Stress and Aneurysm Area Index. *Med Eng Phys.* 2008; 30:329–340. [PubMed: 17556005]
140. Valencia A, Munizaga J, Rivera R, Bravo E. Numerical Investigation of the Hemodynamics in Anatomically Realistic Lateral Cerebral Aneurysms. *Conf Proc IEEE Eng Med Biol Soc.* 2010; 2010:2616–2621. [PubMed: 21096182]
141. Valencia C, Villa-Uriol MW, Pozo JW, Frangi AF. Morphological Descriptors as Rupture Indicators in Middle Cerebral Artery Aneurysms. *Conf Proc IEEE Eng Med Biol Soc.* 2010; 2010:6046–6049. [PubMed: 21097120]
142. van der Kolk NM, Algra A, Rinkel GJ. Risk of Aneurysm Rupture at Intracranial Arterial Bifurcations. *Cerebrovasc Dis.* 2010; 30:29–35. [PubMed: 20424442]
143. Vega C, Kwoon JW, Lavine SD. Intracranial Aneurysms: Current Evidence and Clinical Practice. *Am Fam Physician.* 2002; 66:601–608. [PubMed: 12201551]
144. Wang J, Sun Z, Bao J, Zhang B, Jiang Y, Lan W. Characteristics and Endovascular Treatment of Aneurysms of Posterior Cerebral Artery. *Neurol India.* 2011; 59:6–11. [PubMed: 21339651]
145. Weir B, Disney L, Karrison T. Sizes of Ruptured and Unruptured Aneurysms in Relation to Their Sites and the Ages of Patients. *J Neurosurg.* 2002; 96:64–70. [PubMed: 11794606]
146. Weir B.; MacDonald, RL. Intracranial Aneurysms and Subarachnoid Hemorrhage: An Overview. In: Regarchy, SS.; Wilkins, RH., editors. *Neurosurgery.* New York, NY: McGraw Hill; 1996.
147. Wiebers DO, Torner JW, Meissner I. Impact of Unruptured Intracranial Aneurysms on Public Health in the United States. *Stroke.* 1992; 23:1416–1419. [PubMed: 1412577]
148. Wiebers DO, Whisnant JW, Huston J 3rd, Meissner I, Brown RW Jr, Piepgras DW, Forbes GW, Thielen K, Nichols D, O'Fallon WW, Peacock J, Jaeger L, Kassell NW, Kongable-Beckman GW, Torner JC. Unruptured Intracranial Aneurysms: Natural History, Clinical Outcome, and



- Risks of Surgical and Endovascular Treatment. *Lancet*. 2003; 362:103–110. [PubMed: 12867109]
149. Wong GK, Poon WS. Current Status of Computational Fluid Dynamics for Cerebral Aneurysms: The Clinician's Perspective. *J Clin Neurosci*. 2011; 18:1285–1288. [PubMed: 21795051]
150. Xiang J, Natarajan SW, Tremmel M, Ma D, Mocco J, Hopkins LW, Siddiqui AW, Levy EW, Meng H. Hemodynamic-Morphologic Discriminants for Intracranial Aneurysm Rupture. *Stroke*. 2011; 42:144–152. [PubMed: 21106956]
151. Xu Y, Tian Y, Wei HW, Chen J, Dong JW, Zacharek A, Zhang JN. Erythropoietin Increases Circulating Endothelial Progenitor Cells and Reduces the Formation and Progression of Cerebral Aneurysm in Rats. *Neuroscience*. 2011; 181:292–299. [PubMed: 21376106]
152. Yamaguchi R, Ujiie H, Haida S, Nakazawa N, Hori T. Velocity Profile and Wall Shear Stress of Saccular Aneurysms at the Anterior Communicating Artery. *Heart Vessels*. 2008; 23:60–66. [PubMed: 18273548]
153. Yasuda R, Strother CW, Taki W, Shinki K, Royalty K, Pulfer K, Karmonik C. Aneurysm Volume-to-Ostium Area Ratio: A Parameter Useful for Discriminating the Rupture Status of Intracranial Aneurysms. *Neurosurgery*. 2011; 68:310–317. discussion 17-8. [PubMed: 21135739]
154. Yu J, Wu Q, Ma FW, Xu J, Zhang JM. Assessment of the Risk of Rupture of Intracranial Aneurysms Using Three-Dimensional Cerebral Digital Subtraction Angiography. *J Int Med Res*. 2010; 38:1785–1794. [PubMed: 21309494]

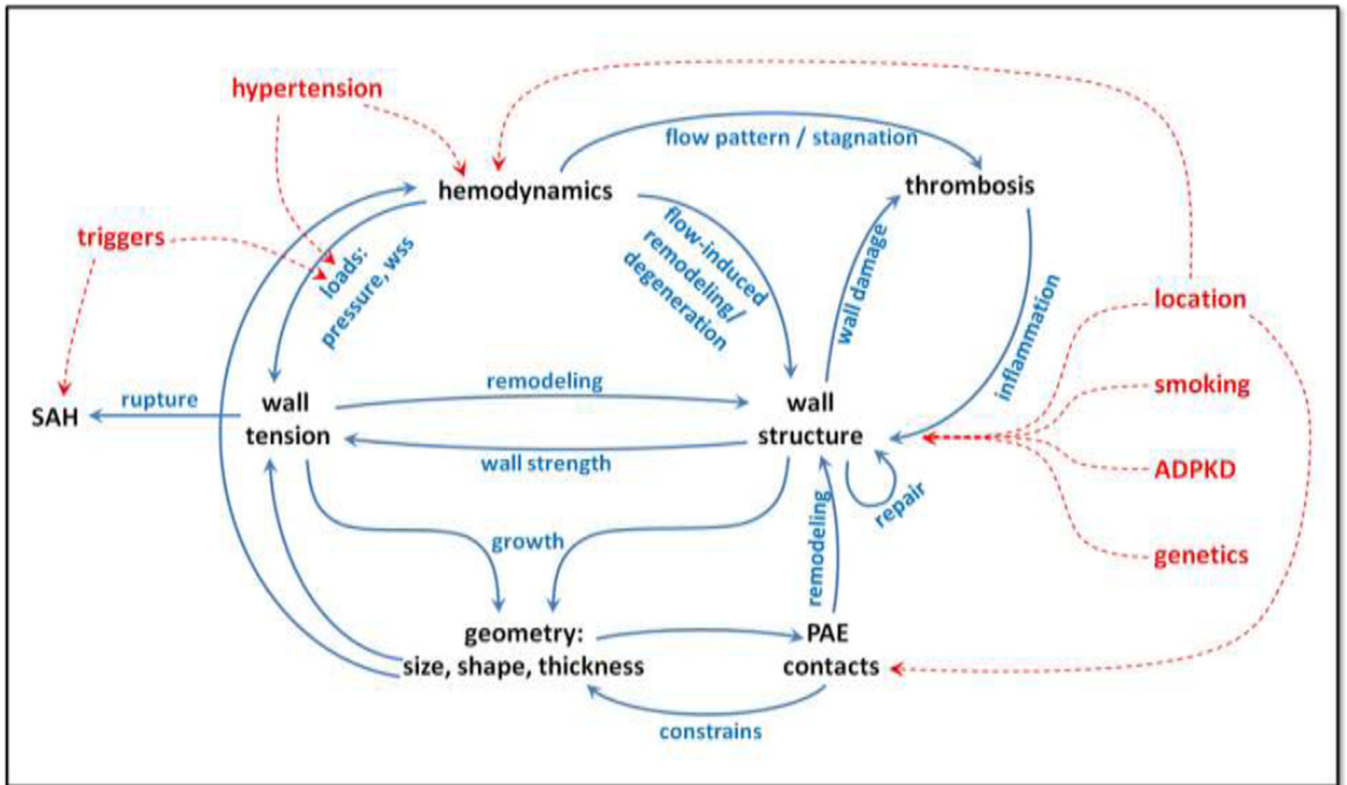


**Figure 1.**  
Intracranial aneurysm risk factors and their interactions.